

Cold Box Upgrade and Commissioning and temperature analysis of pixel modules

Simon Storz

Semester Thesis, ETH Zurich, Institute for Particle Physics IPP
Supervisors: Prof. Rainer Wallny, Andrey Starodumov, Felix Bachmair

July 31, 2014

Abstract

This document describes a Semesterarbeit done at the Institute for Particle Physics IPP at ETH Zürich. It is about commissioning an upgraded cold box which is used to test pixel modules for the CMS detector in it. A step by step guide to calibrate sensor temperature in the box is given. The document contains temperature (and humidity) measurements which show the temperature distribution in the box and on the modules. Furthermore, measurements of the temperature dependency of the leakage current and the DAC parameters of the pixel modules are shown.

Contents

1	Introduction	3
2	CMS Experiment	3
2.1	CMS Detector	3
2.2	Silicon Tracker	3
2.3	Pixel Modules	4
3	Setup	5
3.1	Cold Box	5
3.2	Electronic equipment	6
3.3	Readout	8
4	Cold Box Upgrade	10
5	Measurements	11
5.1	Cold Box: Cooling analysis	11
5.2	Humidity	12
5.3	Temperature	13
5.3.1	Air	13
5.3.2	Base Plate	14
5.3.3	Module Holder	17
5.3.4	Module	18
5.3.5	Comparison	19
5.3.6	Leakage Current	20
5.3.7	Calibration	23
5.3.8	Temperature table	24
5.4	DAC temperature dependency	25
6	Conclusion	27
A	Setup	31
A.1	Conductor Board: Circuit diagram	33
A.2	Python codes	36
B	Measurements	48
B.1	Humidity and air temperature	48
B.2	Base plate	50
B.3	Module Holder	52
B.4	Leakage current	56
C	DAC dependency	59

1 Introduction

This paper is part of a Semesterarbeit done at the Institute for Particle Physics IPP at ETH Zürich. It is part of the Pixel group that works on the upgrade of the CMS pixel detector at the LHC at CERN which is planned for 2017. For the upgrade process every redesigned pixel module which will be installed inside the CMS detector has first to be tested. This is where this Semesterarbeit comes into play. Its aim is to upgrade and commission the cold box where inside the modules later will be tested. An electronic set up is developed to measure temperature and humidity and to easily read out the quantities with a python script. This is used to analyse the temperature and humidity in the cold box in detail. Furthermore, the temperature distribution on module holders and of modules itself are measured in various conditions. Finally, the dependence of DAC parameters on the temperature of the silicon is investigated. The important results are shown and explained in this paper, all data and further graphs can be found in the Appendix.

2 CMS Experiment

2.1 CMS Detector

The CMS experiment is part of the Large Hadron Collider (LHC) at CERN. The LHC basically consists of two 27 kilometre long underground beam pipes in which hadrons are accelerated to a velocity close to the speed of light and will later collide. One of the collisions is done in the middle of the CMS pixel detector. When two hadrons (composite particles held together by the strong force, consist of quarks) collide, some of the energy gained by the collision is turned into mass, namely new particles. The CMS pixel detector is able to detect these resonances with different layers of the detector (figure 1). Most of the particles the scientists are looking for have a very short lifetime when they are created by the energy of the collision. Then they decay in other particles which can be tracked by the detector and give information about the mother-particle (e.g. a Higgs boson) we are looking for. Each of the daughter-particles can be observed in a different layer of the detector: For example the energy of the electron e^- can be measured in the electromagnetic calorimeter (ECAL). A e^- flying through the ECAL deposits energy in form of photon showers in proportion to the energy of the e^- . Hadrons are observed in similar manner in the hadron calorimeter. Muons can fly even through the superconducting solenoid which is used to bend the paths of the particles which are about to collide. Muons are detected in the Muon chambers, neutrinos can not be detected at all. Their presence can be recalculated through missing energy and momentum.

2.2 Silicon Tracker

The Pixel Detector forms the innermost part of the detector. Its aim is to track the path of the particles which are created in the collision of the two protons. This part of the detector provides the best resolution of the path of the particles. The path is bent by a magnetic field. The reconstruction of its radius gives information about the momentum of the particle which is crucial in order to know which particle was involved

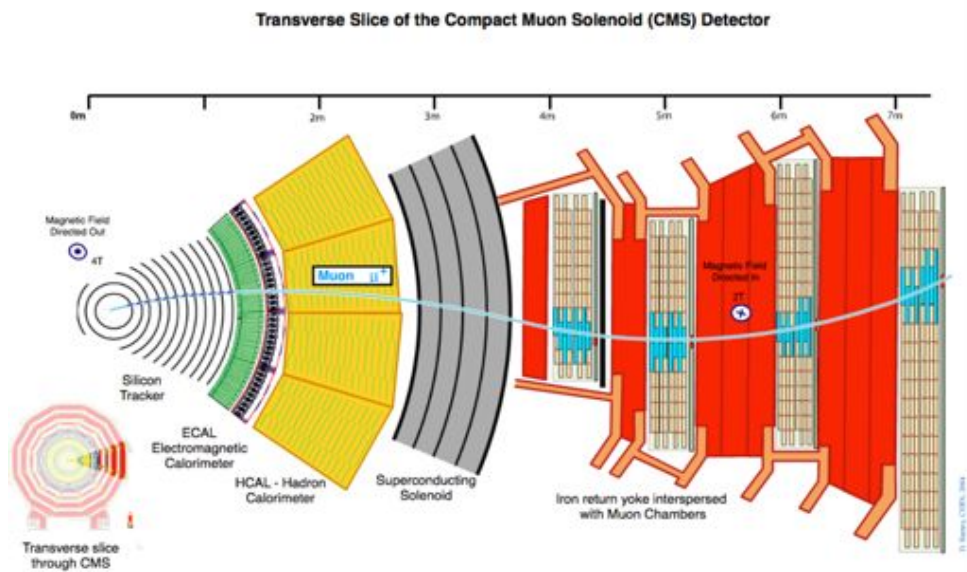


Figure 1: The CMS detector.

in the collision. This way the tracker can reconstruct the paths of electrons, high-energy muons and hadrons as well as short lived decay particles. [1] The pixel detector which is made out of silicon contains 65 million pixels which track the particle's path. There are different layers of readout modules containing these pixels.

2.3 Pixel Modules

One Pixel Module consists of a electronics layer, base strips, a sensor layer and 16 silicon read out chips, each containing 4160 pixels (figure 2). "The silicon sensor is electrically connected to 16 (...) ROCs. The connection between sensor and ROCs is made of indium bumps, which connect each sensor pixel with a pixel unit cell (PUC) on the ROC. On top of the sensor a High Density Interconnect (HDI) serves as an interface to the front end electronics." [4] A charged particle crossing the sensor layer loses energy due to elastic scattering with electrons. Thanks to this energy electron-hole pairs are created in the depleted semiconductor silicon. This causes a small current to flow. These electrons reach the ROCs due to the bias voltage. [4] There the current gets amplified in order that it is enough strong to be measured. [2] At the bottom there are the base strips which are needed to fix the module onto the support.

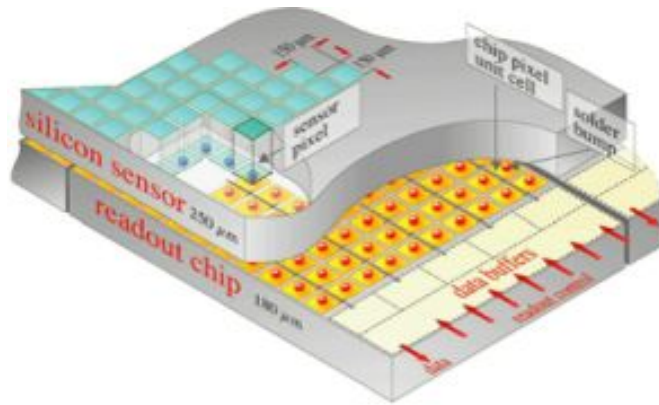


Figure 2: One part of a silicon chip (schematic view) with the sensor layer on top of the ROC.

3 Setup

All experiments related to this Semesterarbeit will be done in the cold box in the clean room of the ETH Institute for Particle Physics IPP. Figure 3 shows the setup with the cold box on the left, an analogue testboard on the top and a Keithley multimeter which powers the module placed in the box.



Figure 3: Experimental setup in the ETH IPP cleanroom.

3.1 Cold Box

The following experiments are done in a Cold Box. This is a machine providing thermal control for a particular volume. With the cold box the thermal circumstances of the CMS experiments are simulated.

The cold box is controlled by the built in JUMO software. The user can program any cooling cycle with the controller in the box or via USB connection with the supervising

software elcomandante. Latter is recommended for long term measurements and if the temperature must be held at a particular setpoint until it is stable.

The cooling of the cold box is provided by four peltier elements which lie directly underneath the base plate (model: QuickCool QC-161-1.6-15.0M 4x4cm). A peltier element consists of two touching semiconductors with different conduction band energy levels. When a current flows, one electron has to absorb energy to jump to the higher conduction band of the other semiconductor. This absorbed energy is provided by thermal energy causing one semiconductor to cool down. The other semiconductor which absorbed the electron gets warmer. This is the cooling effect of the peltier elements. [7] They sit on a copper block in which the water flows. Thanks to the high thermal conductivity of copper, the heat produced by the peltier elements can be dissipated by the water flowing through the block. It is important that the water flow is always on during the cooling process in order not to damage the peltier elements.

Additionally, there is a tube which connects the inner part of the cold box with a dry air filter outside the box. Thanks to that the humidity in the box can be controlled by floating or flushing dry air. It is therefore crucial that every part of the box is well sealed so that no humid air can float into the box. The seal is done with foam rubber, tape, and heavy plumb bricks loading the box (see figure 3) so that the cap is tightly shut.

3.2 Electronic equipment

For the temperature and humidity measurements explained in the following chapters, PT1000 temperature sensors and Honeywell HIH4020 humidity sensors are used. They are connected to a constant current source (DAC/5V), provided by the Labjack. The Labjack is an interface between measurement devices and a computer. It reads the electrical inputs of a connected sensor and sends this information to the computer. The sensors both work in a similar way: The resistance of the sensors (platinum for PT1000) depends on the temperature respectively the humidity of the material. This causes a voltage drop over the sensor that can be measured by the Labjack. The measurement was done with a 4 wire measurement to provide more exact results.

All sensors are connected to a conductor board (figure 4) whose design and construction was one part of this Semesterarbeit. It was developed within 3 versions. For the first measurements (everything until chapter 5.2.4) the second version was used which was self built in the electronics laboratory. The new board (figure 4) was built professionally by the ETH electronics team according to the drawing made with the software eagle that is attached in Appendix A.1. On the bottom of the board it can be connected to the Labjack U6, that converts the analogue voltage signal to a number which can be read out with a computer. In the middle of the plate there are two connectors for sensors providing digital readout by the Labjack. In the middle on the top there is a connector for an analogue readout sensor that provides two output channels. One possibility is to connect a Sensirion SHT75 sensor here measuring temperature and humidity simultaneously. The 12 connectors on the edge of the board are meant to connect with PT1000 and HIH4020 humidity sensors (or others as well). In front of each connector is a jointer that is needed to be covered according to the used sensor type. If a humidity sensor is plugged in, the jointer has to be covered with the part where the "H" (for humidity) is marked. If there is a temperature sensor plugged in, the jointer has to be covered the other way where the

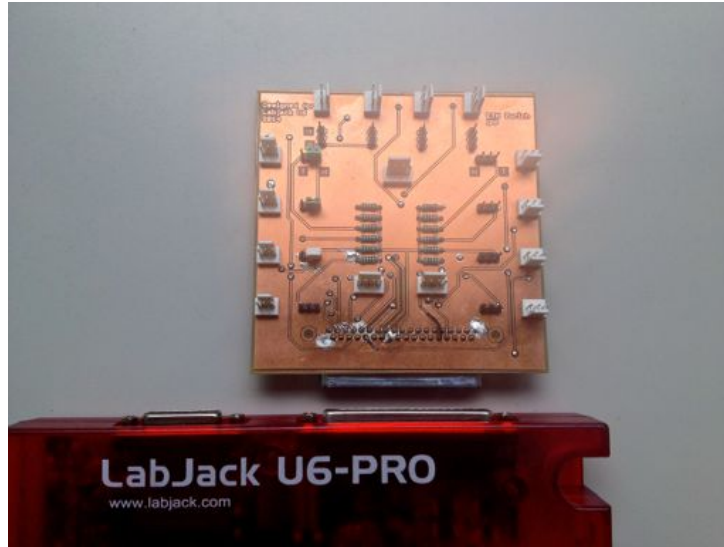


Figure 4: Conductor board with Labjack

”T” (temperature) is written. This is because the sensors are read out differently, which will be explained in the next chapter.

The design of the board makes it possible to measure 16 channels simultaneously. They are numbered from the left (AIN0) to the right (AIN11) plus the middle sensor (AIN12/13). This can also be seen in the attached circuit diagram (appendix A.1). It can be freely chosen how many of these 16 channels are temperature measurements and how many humidity. As figure 5 shows, the sensors correspond very well: the sensors are stuck very close to each other in the box. Then the temperature (resp. humidity) values of each sensor are compared. The PT1000 sensors used for the measurements correspond very good: they differ by 0.2°C . The humidity sensors differ by 1.5%. This inaccuracy has to be taken into account in the humidity map where the gradient is very small anyway (figure 10).

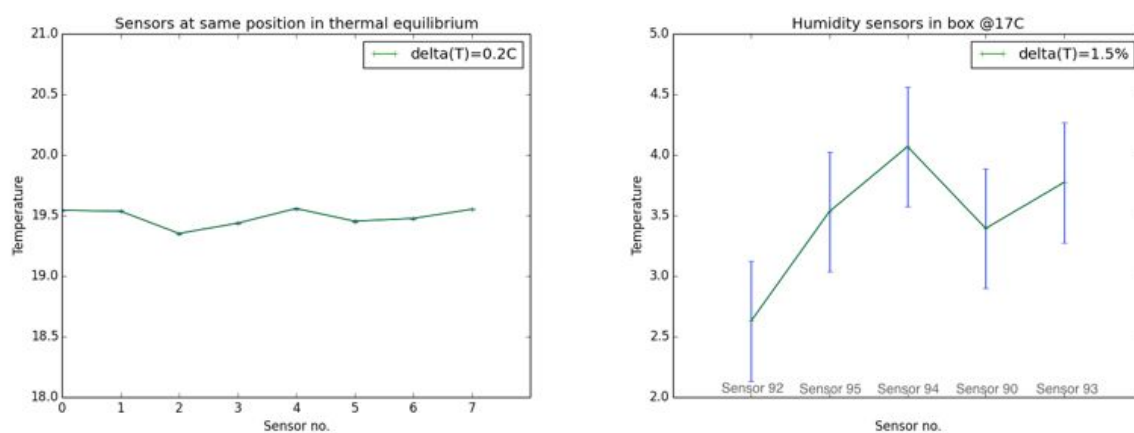


Figure 5: Left: Accuracy of used temperature sensors. Right: Accuracy of used humidity sensors with the corresponding label on the sensor.

The Labjack provides a voltage readout with an accuracy of $\pm 0.01V$. For the old board as well as the new one the resistances of the PT1000 sensors could be read with an accuracy of <1 Ohm which is <1 per mill and corresponds to an accuracy in temperature of $<0.5^\circ C$. Therefore these are the most fundamental inaccuracies on every measurement values that will be shown in this paper and this forms the limit to how exact the data can be measured.

3.3 Readout

As already mentioned the Labjack connected to the board with a DB37 connector converts the measured voltages of the sensors to a number that can be read out with a computer connected with USB. There is a Python module providing commands for the U6 Labjack. There is a difference between the readout of temperature and humidity (see figure 6): For

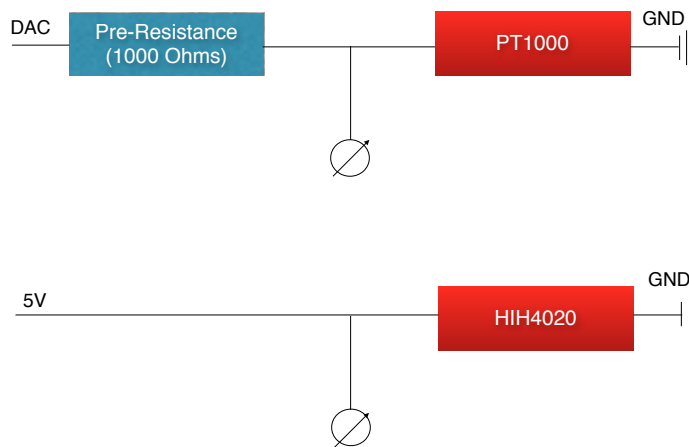


Figure 6: Schematic view of the readout of a temperature sensor (above) and a humidity sensor (bottom).

humidity, the measured voltage is proportional to the relative humidity with the relation:

$$rH = (V_{out} - z)/s \quad (1)$$

where the z =zero offset and s =slope are constants depending on the sensor. With temperature, things are a bit different: There we have a DAC which we set to 0.1 V. But we don't know the exact current yet for each sensor. Therefore an additional resistance which is measured very exactly is placed in front of the sensor and the jointer. Thanks to this the current $I = \frac{R}{v_0 - v}$ can be found. The conversion to resistance goes as follows:

$$R = \frac{v * R_0}{v_0 - v} \quad (2)$$

with the measured input voltage v , the reference resistance R_0 which lies in front of the particular connector and the reference voltage v_0 which has to be measured at one of the connectors while covering the second and third inlet of the connector. This is the reason

why the jointer has to be attached correctly in front of every connector depending on the connected sensor. The resistances are converted to temperatures the following way:

$$T = \frac{a}{2b} - \sqrt{\frac{a^2}{4b^2} - (R - 100)/b} \quad (3)$$

with R = the measured resistance / 10 and the constants $a = 3.902e-1$ and $b = 5.802e-5$ for $R > 100$ and

$$T = aR^5 + bR^4 + cR^3 + dR^2 + eR + f$$

(4)

with R = the measured resistance / 10 and the constants $a = 1.597 * 10^{-10}$, $b = -2.951 * 10^{-8}$, $c = -4.784 * 10^{-6}$, $d = 2.613 * 10^{-3}$, $e = 2.219$ and $f = -241.9$ for $R < 100$. This formula is also used to convert the resistances measured by additional sensors read out by a Keithley multimeter.

All python codes - also the ones for the plots - are attached in the appendix.

4 Cold Box Upgrade

The first aim is to improve the cold box: The new upgraded box should provide a stronger and faster cooling in order to make it as comfortable as possible to work with for upgraded CMS modules testing.

In comparison with the old box several things have changed:

1. First, the diameter of the water tubes are enlarged. The old tubes with a diameter of 9 mm are replaced by others with a diameter of 12 mm (see figure 7). Therefore also the magnetic valve has to be exchanged with one with a larger diameter. Now every part of the box where the water flows has a minimum diameter of 9 mm.

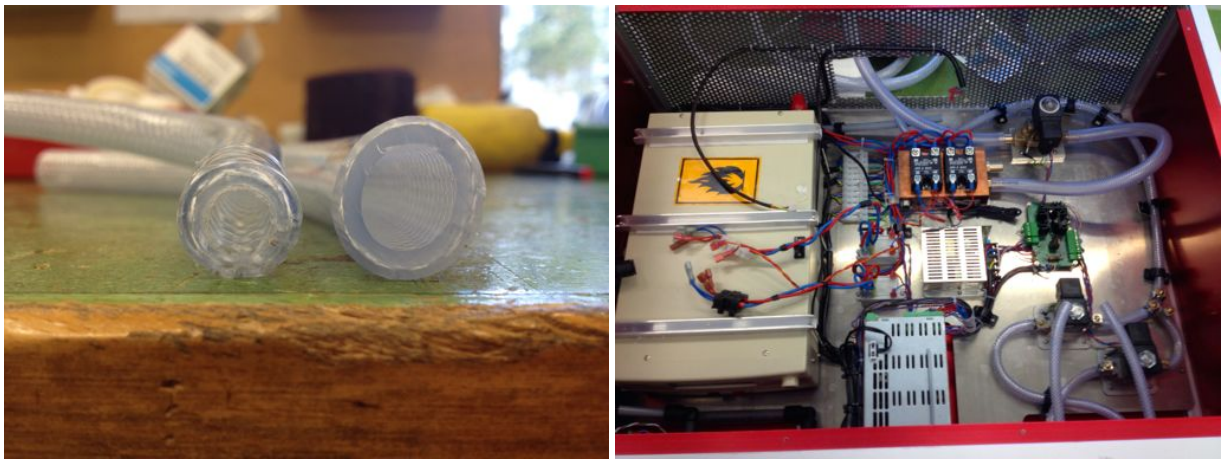


Figure 7: Left: The old (left) and new (right) water tubes in comparison. Right: The inside of the cold box.

Thanks to the larger tubes, the maximal water flow of the box rises to 33.7 l/min. According to the formula

$$\frac{dV}{dt} = v * A \quad (5)$$

with the flow rate $\frac{dV}{dt}$, the velocity v of the water and the cross-section area A , the maximal flow of the old box was 18.8 l/h if the box operated with the same water pressure.

2. Second, a new copper block is installed to the Cold Box. Before, there was only one passage of water in the copper block under the base plate of the box. Now water flows through the copper plate in two parallel pipes having opposite directions.
3. Moreover, new peltier elements are built in. They are as large as before (4x4 cm²). Every part of the cooling box is tightened by cellular rubber, styrofoam and tape to avoid humid air getting in and rising the humidity.

5 Measurements

5.1 Cold Box: Cooling analysis

First, the behaviour of the upgraded cold box is investigated. There are 10 cycles programmed for the analysis of the cooling process of the box: In each cycle, the box cools down to -20°C and afterwards heats up to $+20^{\circ}\text{C}$ while flushing dry air. As figure 8 shows, the temperature rises beyond the $+20^{\circ}\text{C}$ setpoint in each cycle. This shows that it takes about one minute until the box gets colder again. This is because the material and the air need some time to transport the colder atoms to the JUMO sensor. Moreover the relative humidity always stays between 5 and 10 % and lowers during the multiple cycle process which is a good result for further module testing in the box.

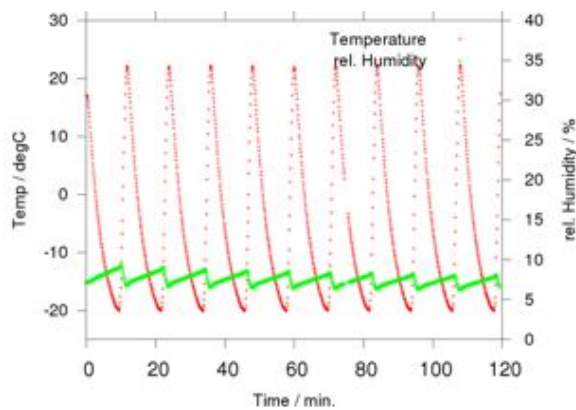


Figure 8: 10 temperature cycles in the new Cooling Box

Figure 9 shows one cooling process in detail for the setpoint values -20°C and -25°C . The new cold box reaches a stable level of -20°C in 12 minutes and -25°C in 20 minutes. The lowest reachable temperature is -27.5°C . We see from this results that the upgraded box can cool faster and to a lower temperature than the old box. There it took 16 minutes to cool to -20°C , a cooling to -25°C was not possible.

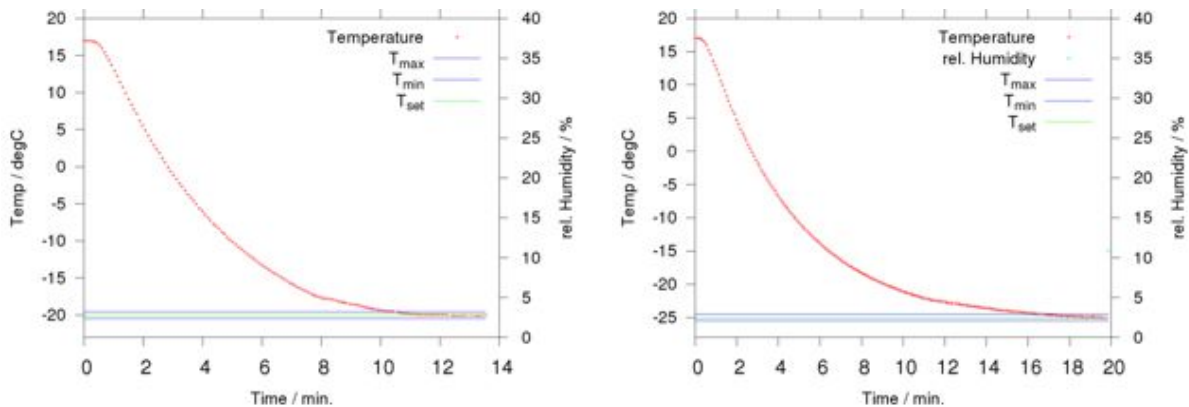


Figure 9: Cooling to setpoints -20°C and -25°C

5.2 Humidity

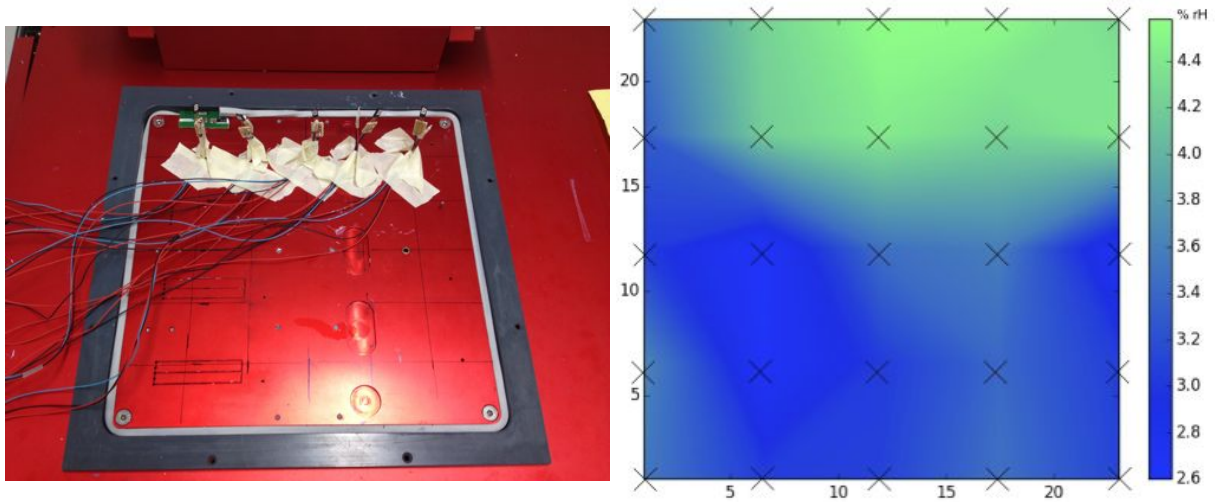


Figure 10: Left: Humidity sensors in the cold box. Right: Humidity map for setpoint temperature -25°C .

Now the box and the electronic equipment is used to measure thermal quantities of the setup. First we have a look at relative humidity in the cold box. This is measured with Honeywell HIH4010 sensors as seen in figure 10 (left). The sensors are placed 4.5 cm above the base plate, which is $1/3$ of the total height of the cold box. Totally 25 points are measured. First, the box is floated with dry air until the Jumo sensor reached a humidity level of 9%. Then the box is cooled down to -25°C . The measurement is started as soon as the temperature in the box is stable. For humidity, 100 measurements are done for each sensor. Then the mean value is taken. The corresponding relative humidity map is pictured in figure 10 (right). The humidity varies by 1.7% within the box. It can be observed that the rearward part has a higher relative humidity than the other parts. First it has to be mentioned that this can not be caused by a particular sensor not working well because the measurements are done row by row (not column by column). There are two possible explanations why the rearward part has a higher relative humidity. First, the sealing between the cap and the base plate could be not perfect, so some humid air may come in there. As the air in the box is colder than the air outside the air pressure outside is higher. It is estimated that this thermal effect is stronger than the floating dry air (60l/h) in the box rising the pressure inside. Therefore there is a possibility that there is a small leaking at the rear. The alternative explanation is that the dry air does not float rectangular to the base plate into the box. This small angle causes the air to come to the front part of the box first, causing the more humid air to float to the rearward part. This explanation is consistent with the map of the air temperature shown in the next chapter.

In any case a minor redesign of the box should be considered. On the one hand it has to be ensured for future box upgrades that the dry air floats perfectly rectangular into the box. This could be achieved by fixing the air tube better to the base plate and to look that the tube is not bended too strong before the connection to the base plate. On the other hand the mechanism of the cap could be reconsidered. The problem with a

possible leaking is a common one and could be resolved by changing the way the cap is fastened to the box. Now it is folded from the bottom to the front. The sealing could be improved by tightening the cap to the base plate. This could be done with screws or another tightening mechanism.

5.3 Temperature

5.3.1 Air

The air temperature in the box is measured simultaneously with the humidity. Therefore, the positions (4.5 cm above the base plate) as well as the initial conditions of the measurements are the same as described above.

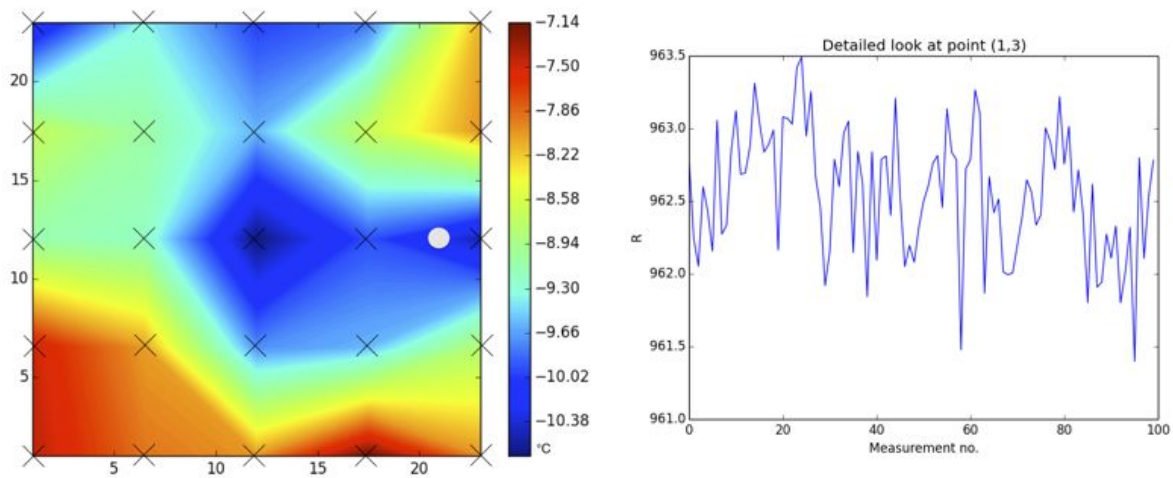


Figure 11: Left: Temperature map of the air temperature at 4.5 cm above the base plate of the cold box. Right: All measurements of the point in the 4th row from the top, 5th column. No trend can be seen, the measurements fluctuate around a mean value.

The air temperature distribution is shown in figure 11. The temperatures are on average 15°C higher than on the base plate underneath (setpoint -25°C; see chapter 5.2.2). $\Delta(T)$ is 3°C. As figure 11 (right) shows this is a map which is not only valid for a few seconds: The 100 measurements of the points (which took about 3 minutes) fluctuate around the mean value which is shown in the map. This indicates that the situation shown in figure 11 is stable. The standard deviation on the values is $\leq 1.1^\circ\text{C}$. The white point shows the position where the dry air flows into the box. The mean dewpoint at 4.5 cm height in the box is $-41.5 \pm 2.2^\circ\text{C}$ according to the measurements with the Labjack. This corresponds well with the dewpoint calculated from the temperature and humidity value the Jumo sensor measured: Here the dewpoint is $-43.2 \pm 1.1^\circ\text{C}$. The formula for the dewpoint calculation is:

$$T_{DP} = c * \frac{y}{b - y} \quad (6)$$

with

$$y = \ln\left(\frac{rH}{100}\right) + b * \frac{T}{c + T} \quad (7)$$

and $b = 17.67$, $c = 243.5^\circ\text{C}$. In addition, it can be seen that the temperatures in the front of the box are much higher than on the other parts. This could again be explained by the

non rectangular dry air tube. This causes warmer air to flow to the front parts of the box and explains why we measure a low air temperature at the position where the air comes in. Nevertheless, more investigations on the air temperature are recommended.

5.3.2 Base Plate

For this part, the number of measurement points is increased to a 7x7 map of the temperatures on the base plate of the cold box. The PT1000 sensors were stuck to the base plate with thermal paste and tape as shown in figure 12 (left). 150 measurements are done for each sensor. First, the box is flushed with dry air until the Jumo sensor shows a humidity value under 9 %. Then the cooling begins. The measured temperature distribution is what was expected: In the middle parts where the peltier elements are, the coolest temperatures are observed. In the measurement with setpoint $-25\text{ }^{\circ}\text{C}$ (figure 13), the base plate gets here even colder than the setpoint value. From the middle to the left and right border we see that the temperature steadily increases. This effect is stronger on the right side of the box ($\text{delta}(T) = 6\text{ }^{\circ}\text{C}$; left side: $\text{delta}(T) = 5\text{ }^{\circ}\text{C}$) and it is stronger at colder setpoint temperatures. These measurements correspond very well with those of Brian Kaputska [5] with the non-upgraded cold box. The standard deviation on the values are $\leq 1.5\text{ }^{\circ}\text{C}$ for each measurement point and $\leq 4.2\text{ }^{\circ}\text{C}$ for the points in the middle on top of the peltier elements. This is a gradient we expect to see. In contrary the $\text{delta}(T)$ in the vertical direction is something we want to have as low as possible. It is $0.5\text{ }^{\circ}\text{C}$ at the outer parts and $1.5\text{ }^{\circ}\text{C}$ in the middle where the peltier elements are. The gradient is bigger in the middle because during the 150 measurements which take about 5 minutes the peltier elements do not cool constantly. Their cooling depends on the Jumo sensor which forces them to stop cooling if the temperature falls under the setpoint and vice versa. All in all these are good results: They show that the temperature distribution on most parts of the base plate of the upgraded box is much more homogeneous than within the old box. There a vertical $\text{delta}(T)$ of $0.8\text{ }^{\circ}\text{C}$ was measured [5].

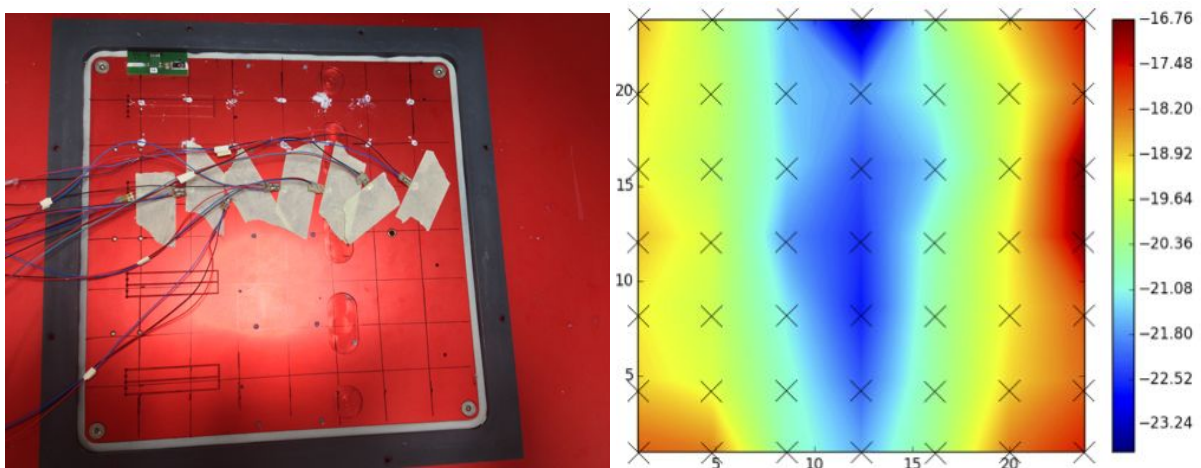


Figure 12: Left: Temperature measurement on the base plate with 7 PT1000 temperature sensors. Right: Temperature map of the base plate at setpoint $-20\text{ }^{\circ}\text{C}$.

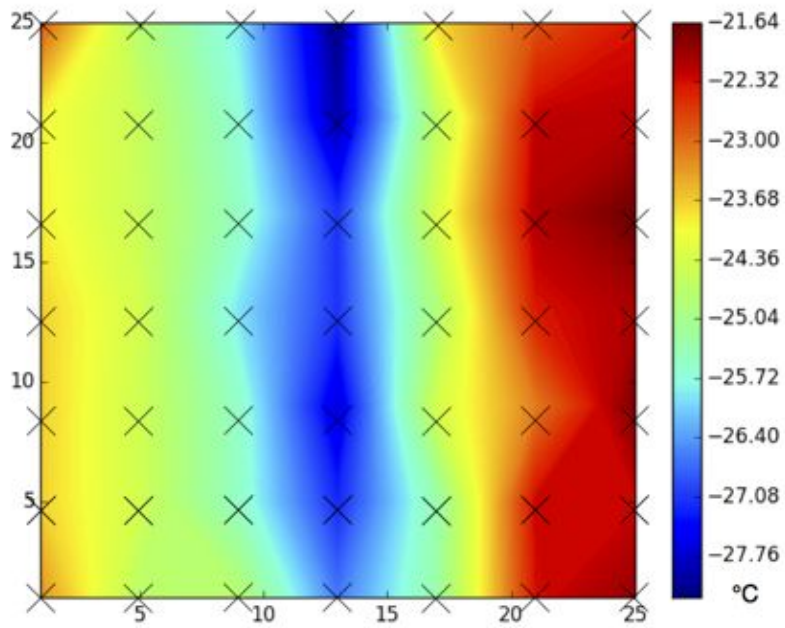


Figure 13: Temperature map of the cold box base plate at setpoint -25°C . The measurement points are marked with crosses.

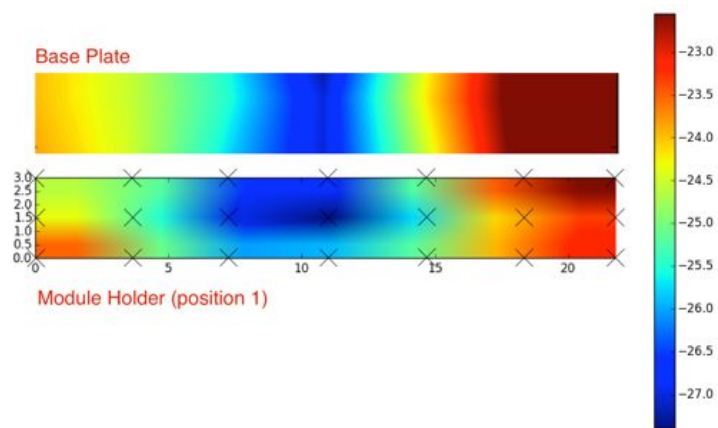


Figure 14: Temperature distribution of the red module holder in the cold box at position 1 and setpoint temperature -25°C .

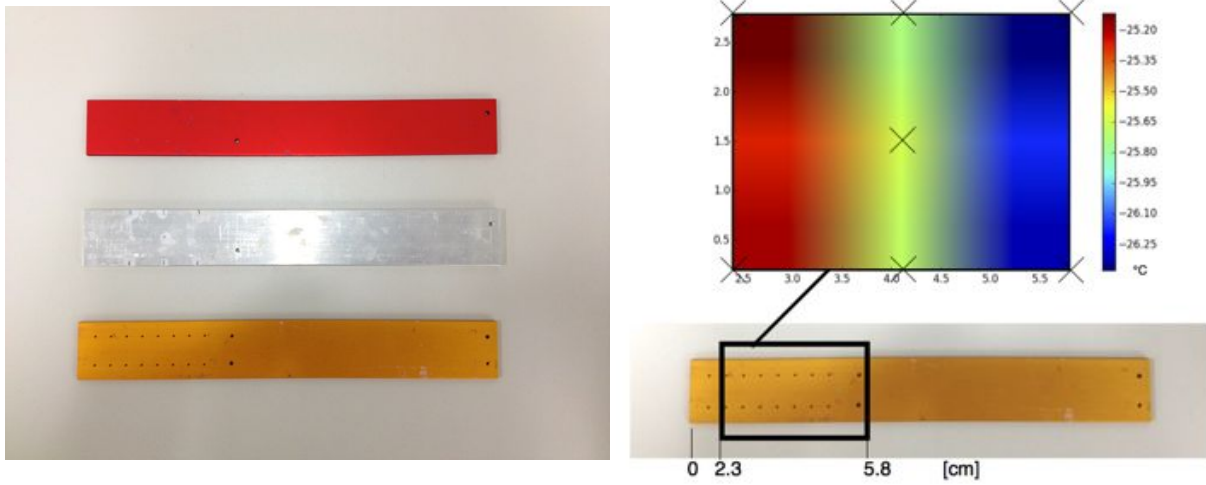


Figure 15: Left: The 3 tested module holders. Right: Exact measurement of red module holder at module position and position 1 in cold box. Setpoint: -25°C .

5.3.3 Module Holder

In this part we are interested in the temperature distribution on the module holders on which pixel modules later will be tested. For that we make several different measurements:

First, the temperature of one module holder is measured on every part of the holder. For that, the red module holder (see figure 15 right) is placed on position 1 in the cold box (2nd from the top). Then the box is cooled down to -25°C . Now the temperatures of 21 measurement points on top of the module holder are taken. As the heatmap in figure 14 shows, the total temperature gradient is 5°C . As expected we observe that the coolest part of the module holder is in the middle where the peltier element lies underneath. The temperature gradient between the middle and the outer parts look very similar to the distribution on the base plate (figure 13). The error on the values are $\leq 1.2^{\circ}\text{C}$. One has to take into account that the measurement on this particular area of the base plate is not very exact which explains the more detailed structure of the module holder temperature map.

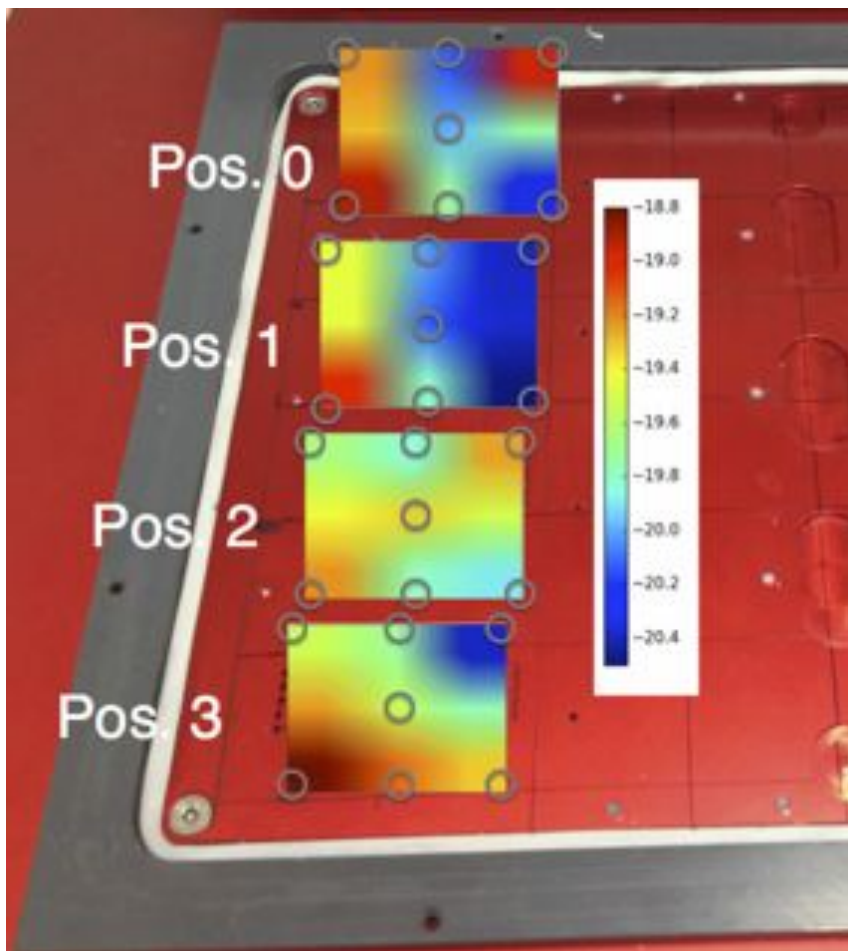


Figure 16: Temperature dependence of the yellow module holder on the 4 positions in the cold box.

From now on, we concentrate on the part of the module holder where the module will later be placed. We want to compare this area of interest later with other measurements of the module base strips. First, an exact measurement of this part on the red holder is taken (figure 15).

No module is installed on the holder. The part we are looking at begins at the module holder length of 2.3 cm and ends at 5.8 cm. We observe a temperature gradient of $1.2^{\circ}0.63\text{C}$ in this area. The left part is the warmest, the right border is the coldest. This measurement is done without any other module holders in the box. The temperature on the module holder increases by 1°C if 3 other (red) holders are inserted into the box. One could say that the thermal energy in the box is distributed to the three other holders as well causing the first one to cool down a bit. The corresponding heatmap is attached in appendix B.3.

Next, the temperature dependence on the module holder material and thickness is investigated.

So far, all measurements are done with the red holder. We now repeat the temperature measurement of the area where the module later will be installed with the two other stainless aluminium holders (figure 15 left). The silver holder is 1.15 mm thicker than the others (4.15 mm: silver holder. 3.0 mm: Red and gold holder.). The gold and red holders are anodized. The temperatures on particular positions on the different holders vary by 0.5°C which is within the standard deviation on the individual temperature measurements ($\leq 1^{\circ}\text{C}$). It can be said that it does not make a significant difference in temperature if another module holder is used. The detailed color maps are attached in appendix B.3.

Finally, it is of great interest whether the temperatures on the module holder differ between the 4 positions in the box. Therefore, the temperatures are measured on the yellow holder on the 4 different positions in the box. The results are shown in figure 16. Position 2 is the one with the smallest temperature dependence. All in all a temperature gradient of maximal 1.2°C can be observed. The only point with a temperature gradient of more than 1°C is the upper right corner. The other points vary with less than the standard deviation ($\leq 1^{\circ}\text{C}$) on the temperature values which shows that the gradient between the positions is not significant.

The temperature distribution on the holder itself reproduces very well the distribution on the base plate which is what we expect to see. The measurements on the module holders also show that there is only a small difference in the temperature distribution if we change something in the setup (position, holder, insert other holders). This is an important information for the operation of the box and further tests of the pixel modules.

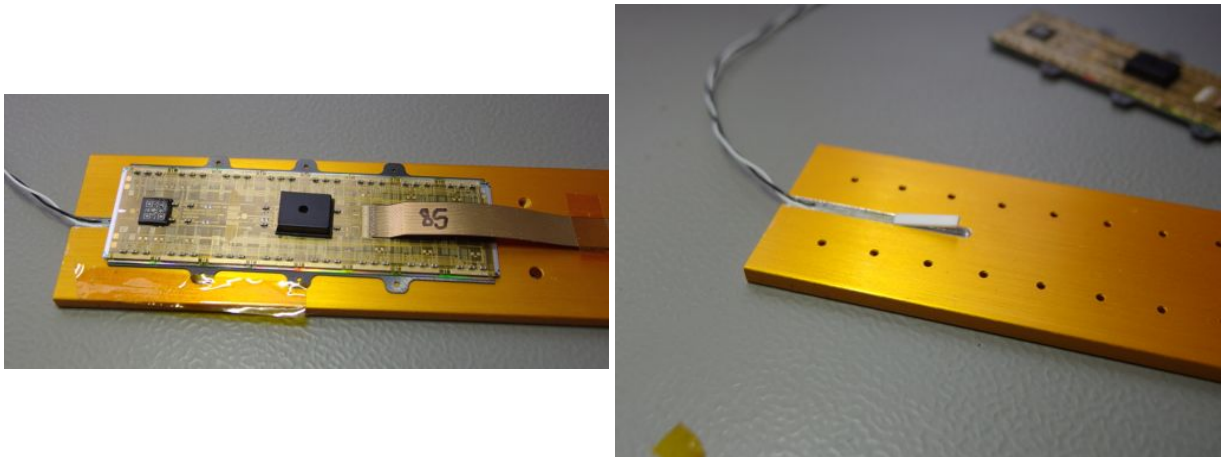


Figure 18: Module holder with PT1000 temperature sensor underneath and module on top of it.

5.3.4 Module

In this chapter, the temperature on powered modules are observed. A module is put onto the yellow module holder. In fact for the following experiments, a slightly different

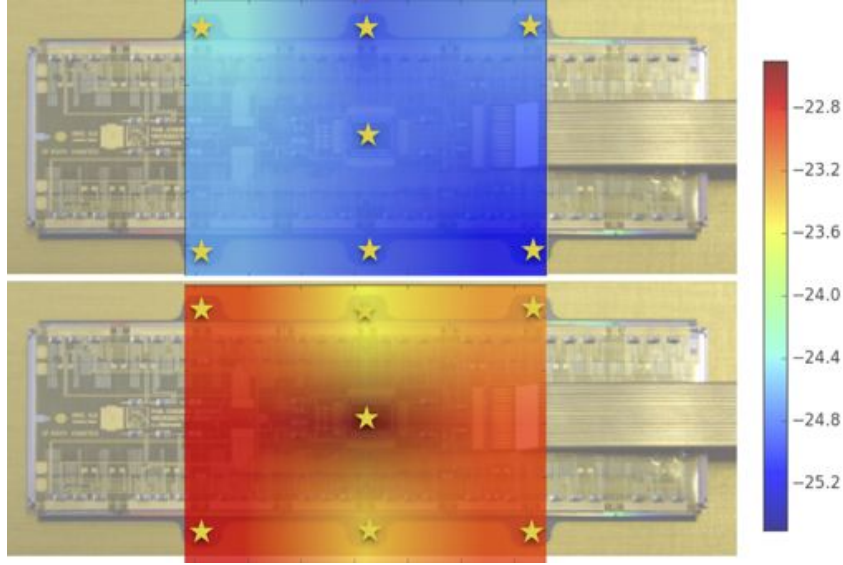


Figure 19: Temperature distribution on module with unpowered ROCs (above) and powered ROCs (below).

module holder is used (see figure 18).

It has a built in PT1000 temperature sensor which lies underneath the middle of the module and measures the temperature on the bottom of the module.

To compare all the measurements later, again a setpoint of -25°C is chosen. For the first part, the module is powered, but not the ROCs. The temperature is measured on the 6 holders of the base strip of the module, as seen on figure 17. Furthermore, the PT1000 sensor under the module is taken into account. Thus there are totally 7 measurement points. The PT1000 sensors are stuck onto the 6 base strip holders with conductive paste. Then the sensors and therefore the whole module are pressed with captain tape against the module holder. In the second part the ROCs get powered. After waiting about 10 minutes, the second measurement is done. The results are illustrated in figure 19 and show that the mean temperature increases by 1.7°C (error $\leq 1^{\circ}\text{C}$) when the ROCs are powered. This is caused by the current heating up the silicon material of the ROCs which heats up the base strips.

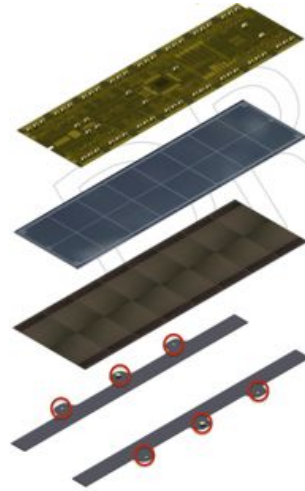


Figure 17: CMS Pixel module. The red circles represent the measurement points of the PT1000 sensors.

5.3.5 Comparison

Now it is possible to compare the different steps. We are interested in the temperature distribution of the whole setup. This is illustrated in figure 20. It can be seen that the mean temperature of the base plate and the module holder at the shown position is

the same, but the temperature gradient on the module holder is much smaller and more homogeneous. From the module holder to the base strips a small temperature increase of 0.4°C is observed. When powering the ROCs we see another temperature increase on the base strips of 1.7°C , which is much higher than the inaccuracies on the temperature values and therefore significant. All in all a mean temperature gradient of 2.1°C is measured on the same position between the base plate and on the module base strips.

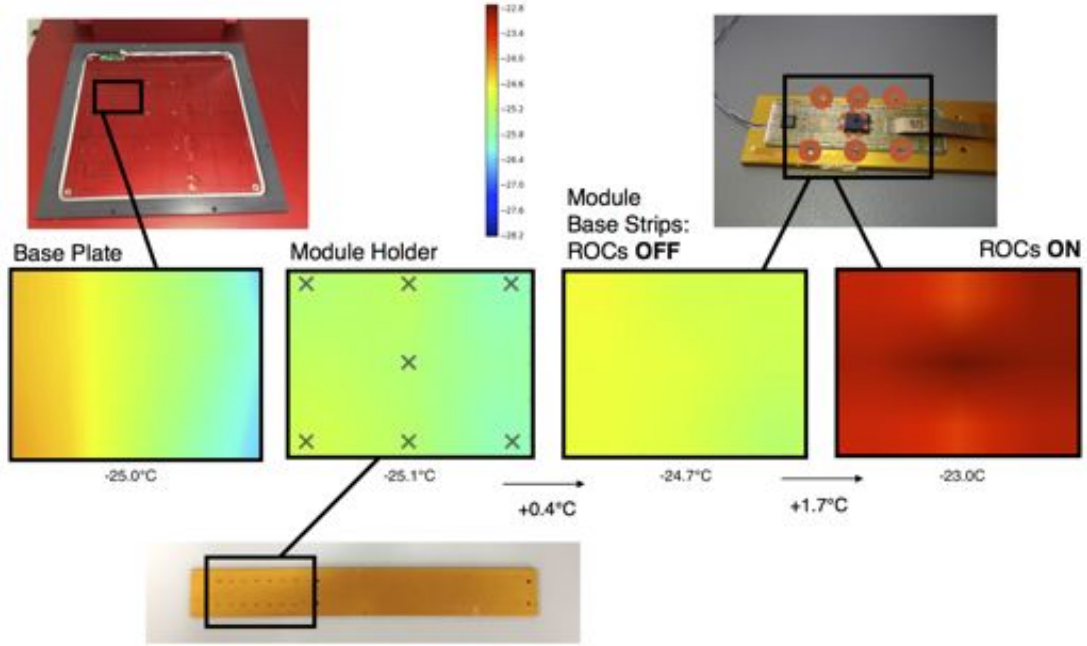


Figure 20: Comparison of the temperature distribution on a) the base plate at the area of interest b) the important part of the module holder c) the module base strips with unpowered ROCs c) with powered ROCs. All measurements were done under the same conditions, positions and with a setpoint of -25°C .

5.3.6 Leakage Current

The leakage current which powers the module strongly depends on the temperature of the silicon material:

$$I_{Leakage} = I_0 T^2 e^{-\frac{E_G}{2k_B T}} \quad (8)$$

with the band gap energy of silicon $E_G = 1.11 \text{ eV}$ at $T = 302\text{K}$ and the calibration constant I_0 which depends on the sensor and the setup. The calibration constant can be found with the sensor calibration which is described later. Here a constant of $I_0 = 0.018$ was found. The calibration constant can also be found more accurate by including the temperature dependency of I_0 :

$$I_{Leakage} = I_{L,reference} * \frac{T}{T_{ref}} * e^{-\frac{E_G}{2k_B} * (\frac{1}{T} - \frac{1}{T_{ref}})} \quad (9)$$

Here, $I_{L,reference}$ is the leakage current measured at a reference temperature (described in chapter 5.3.7) and T_{ref} the corresponding sensor temperature read out with the PT1000

touching the ROCs. This more detailed calculation does not change the results much as figure 22 shows: The slopes of the interpolation lines differ only by 0.004. All in all it shifts the temperature values by 0.5°C to lower values.

First it is of great interest to look at the long-time behaviour of the leakage current at a particular JUMO setpoint. In figure 21 it can be seen that it takes about 5 hours to reach a stable leakage current if the box and the module are set to thermal equilibrium. If the box is set to a particular setpoint, it takes much less time (approx. 20 min) to have a stable leakage current flowing through the module. This is important for the calibration part that will be explained later. After the leakage current has got stable, the current remains constant. Further data is attached in the appendix.

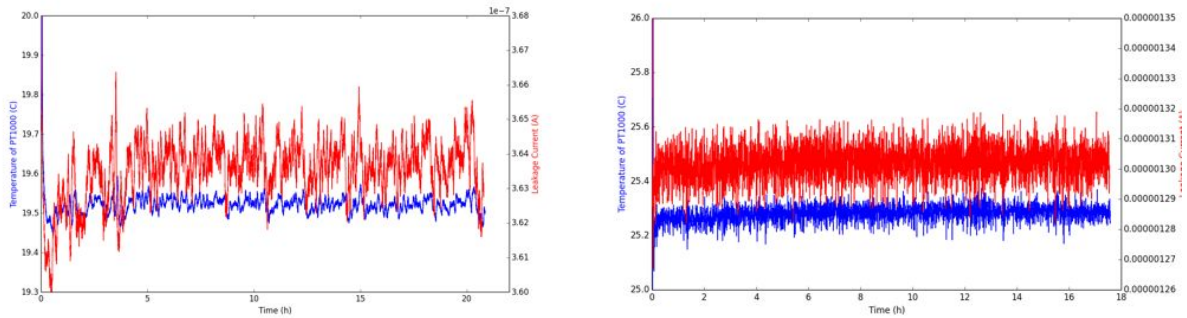


Figure 21: Left: Behaviour of the leakage current in thermal equilibrium with unpowered ROCs. Right: Behaviour at a JUMO setpoint of $+17^{\circ}\text{C}$ with powered ROCs.

Now three temperatures are compared: The one measured by a) the JUMO sensor on the bottom of the cold box base plate b) the ROCs temperature measured by the PT1000 sitting underneath the tested module and c) the sensor temperature which is read out from the leakage current via formula 8 (figure 22). The whole measurement was done twice, giving slightly different results. The slopes of the interpolation lines between the two measurements only differ by 0.009, but there is a remarkable shift to lower temperatures ($\Delta(T)=-2.5^{\circ}\text{C}$) in the value of the sensor temperature in the second measurement. Such a corresponding shift is also seen on the values of the ROC temperature represented by the PT1000 underneath the module ($\Delta(T)=-1.5^{\circ}\text{C}$). The two measurements were done with exactly the same conditions. It is not yet fully understood why the two measurements differ that much. One possibility could be that the module was already working a few hours before the first measurements were done. This could have caused the silicon to be much warmer from the beginning. The second measurement was done on another day where the module has not been used before for several hours. The problem that the leakage current differs from measurement to measurement is also discussed later in this chapter in correlation with reproducibility. It is important to see that the slopes of the two measurements do not differ much and that the difference is only caused by a constant shift. Nevertheless the second measurement is preferred because of the explanation above and the fact that it agrees much better with the temperature measurements from chapter 5.3.4 than the first measurement. Also shown in figure 22 is the calibration point in green, with which the calibration of formula 8 was done. More graphs can be found in Appendix B.4.

The leakage current differs whether the ROCs are powered or not. As seen before an

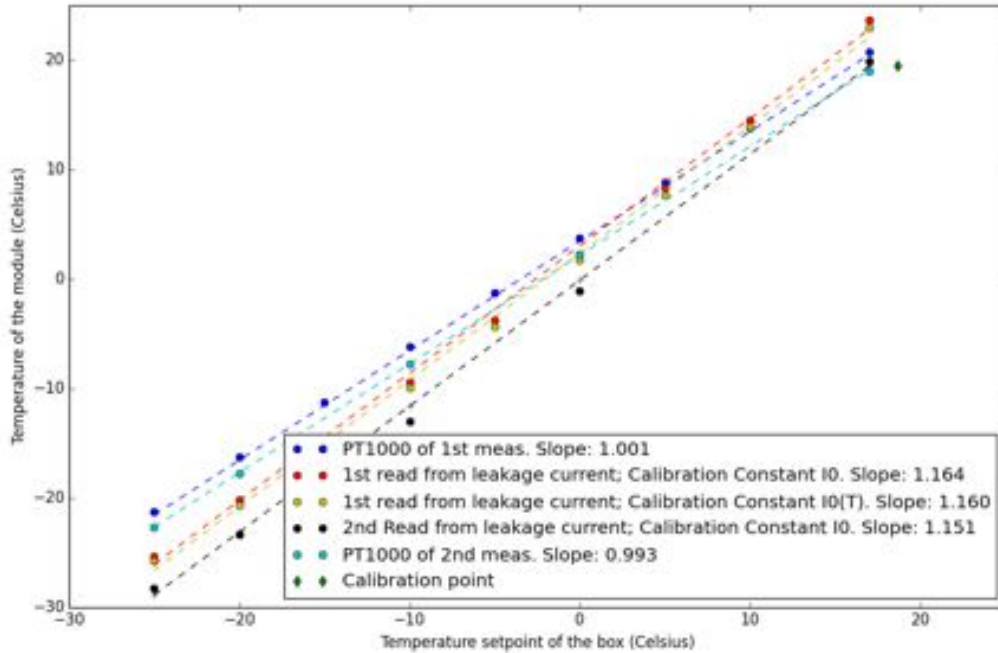


Figure 22: Temperature converted from leakage current, PT1000 underneath the module and JUMO sensor compared at different JUMO setpoints. ROCs power on.

increase in temperature is observed when the ROCs get powered. This measurement is done with the PT1000 sensors on the base strip. Now similar results can be found for the silicon sensor material by looking at the leakage current (and the converted temperature) of the module at a setpoint of $+17^{\circ}\text{C}$ in the box (figure 23). First, the ROCs are unpowered. Then suddenly the ROCs get powered and the leakage current rises by $7.5 \cdot 10^{-8}$ A. This corresponds to a temperature increase of 2.6°C from 17.1°C to 19.7°C . Comparing these results with the temperature rise of the ROCs it can be seen that this part of the sensor heats up less ($+1.4^{\circ}\text{C}$) than the silicon which affects the leakage current. This agrees with the bigger slope of the silicon seen in figure 22.

Moreover, it is also observed how good the results from the leakage current measurements can be reproduced. The first part is to start the measurement of the leakage current (JUMO setpoint: $+17^{\circ}\text{C}$, ROCs powered), wait for 45 minutes, note the measured stable leakage current, and stop the measurement. Then without any setup changes, do the same again. The result of this reproducibility measurement is that the measured leakage current values differ by $0.5 \cdot 10^{-7}$ A which corresponds to a temperature of 1.05°C . The second part is to open the cold box, lift the module holder with the module on it and to put it down again at the same position (1) between each measurement. This is to investigate whether there is an influence on the temperature if the module holder is not perfectly flat and lies differently on the base plate each time. Here it can be seen that the leakage current differs by $0.7 \cdot 10^{-7}$ A each time (1.7°C). There is one measurement (the first one) which gives much higher results than all other four and was therefore not

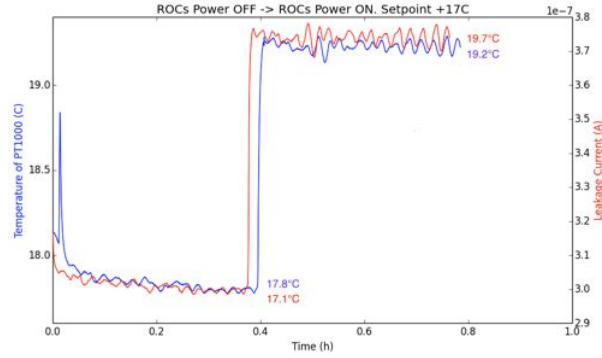


Figure 23: ROCs first unpowered and then powered. Setpoint: +17°C.

taken into account in this calculation. Probably something with the module changed after this first measurement, causing all following ones to measure lower currents. The detailed graph can be found in the appendix.

The leakage current measurements show that the temperatures of the silicon sensor material is 3.3°C lower than the JUMO sensor and 5.5°C lower than the temperature of the ROCs at a setpoint of -25°C. In addition it has been shown that one has to wait for 20 minutes until any tests with pixel modules should be started in the cold box, using any particular JUMO setpoint. There it does not have an influence whether the ROCs are powered or not. If the box is set to thermal equilibrium, the leakage current and therefore the sensor temperature needs 5 hours to get stable. This only works for unpowered ROCs as there are breakthroughs of current observed when the ROCs are powered (see Appendix B.4), causing the current to not get stable at all.

The results of the sensor temperature measurements are not what was expected to see and are not fully understood yet. They could be observed in more detail in further investigations.

5.3.7 Calibration

After installing a new cold box it is important to calibrate the sensor temperature and the leakage current before measuring anything that has to do with temperature corresponding to the current of the module. This is how to do the calibration:

1. First, the calibration point has to be found. Therefore, a module has to be installed in the cold box. Power the module, but not the ROCs.
2. Close the box and set it to thermal equilibrium: Water flow (33-44l/h), dry air flow (approx. 60l/h), setpoint: 40°C to prevent the peltier elements from cooling.
3. Now track the leakage current and the resistance of the PT1000 underneath the module with elcomandante for some hours (see figure 21 (left)). Therefore the bias voltage has to be set to -150V provided by a Keithley multimeter connected to the testboard. It is important to be sure to have reached a stable thermal equilibrium and therefore a stable leakage current in the box before moving on. Now, the PT1000 temperature under the module and the temperature converted from the stable leakage current should correspond well. We assume that now the ROCs and the sensor

have the same temperature because they are in thermal equilibrium. The temperature of the PT1000 is read out by another Keithley and tracked with elcomandante. It can later be converted to a temperature. The calibration measurement done for this Semesterarbeit gives the following data: JUMO sensor temperature: 18.65°C; temperature of PT1000: 19.45°C; $I_{Leakage}=3.65e-7$ A.

4. Now the sensor constant in formula 8 can be found inserting the measured leakage current $I_{Leakage}$ and for T the temperature measured by the PT1000 under the module. This gives I_0 .
5. From now on temperature conversions from the measured leakage current should be calibrated. This can be tested the following way: turn on the ROCs power. Set several JUMO setpoints between +20°C and -25°C (e.g. steps of 5°C). For each measurement the leakage current is measured and compared with the values of the PT1000 (figure 22). Important: Before each measurement one has to wait until the leakage current gets stable. This takes (see figure 21 right) about 20-30 minutes.

5.3.8 Temperature table

On the table below the different measurements are shown and can be looked up. BP = base plate; MH = module holder; BS = module base strips. The listed measurements with powered modules are all made with ROCs power on. The data of the base strip and module holder measurements show the part where the module sits on (position 1 in the box) as shown in figure 20. The listed base strip temperature data is taken from the corresponding heatmaps and shows the mean values of the left, middle and right part of the area. The temperature gradient is very small in the y direction and only in x direction in this area of the plate. The data of the module holder measurements are mean values of each two measurements (up & below) for the left, middle and right part of the yellow module holder (as shown in figure 15 left) with a detailed measurement of the yellow holder which is attached in the appendix. The values of the base strip temperatures are calculated in the same way as before, but with the data of the measurements in figure 19 (below). The Temperature values of the ROCs of the sensor which are measured by the PT1000 sensor built in the module holder (figure 18) are also listed. Finally the temperatures of the silicon sensor are converted from the leakage current measurement shown in figure 22. The converted temperatures and the leakage current (in Ampere) are listed. It can be seen that when the JUMO sensor of the box shows -25°C, this is also the mean temperature on the position of interest on the base plate. There is no significant temperature gradient between the base plate and the module holder. But there is small one (0.4°C) between the module holder and the base strips. With powered ROCs the gradient is even bigger (approx 2°C). With a setpoint of -25°C the powered ROCs reach a temperature which is about 2.3°C warmer than the JUMO setpoint. The delta(T) between the JUMO sensor and the sensor material is -3.3°C.

JUMO temp	BP left	BP middle	BP right	MH l	MH m	MH r	BS l	BS m	BS r	ROCs temp	Sensor temp	Leakage c.
17	-	-	-	-	-	-	-	-	-	19.9	> 19.9	3.8e-7
0	-	-	-	-	-	-	-	-	-	2.18	-1.1	5.9e-8
-10	-	-	-	-	-	-	-	-	-	-7.82	-13.0	1.8e-8
-20	-19.4	-19.7	-20.4	-19.3	-19.9	-20.3	-	-	-	-17.7	-23.4	5.9e-9
-25	-24.4	-25.0	-25.9	-24.5	-25.15	-25.7	-23.1	-23.58	-22.95	-22.77	-28.3	3.35e-9

5.4 DAC temperature dependency

In this chapter the dependence of the DAC parameters on the temperature which control the ROCs is investigated. A module is placed inside the cooling box. With elcomandante, several tests are set: Pretest at 17°C, Pretest at 10°C, Pretest at 0°C, Pretest at -5°C, Pretest at -10°C, Pretest at -15°C, Pretest at -20°C, Pretest at -25°C. In each step, the box cools down until a stable setpoint is reached. Then the pretest optimises the DAC parameters for the corresponding temperature in the box. The data is stored and can later be compared:

There are only 5 out of 21 DAC parameters which change with temperature. This can be

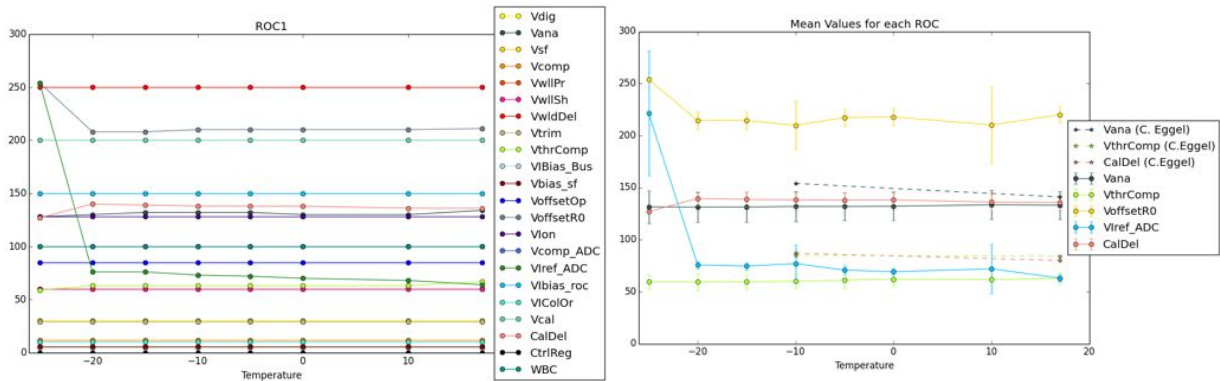


Figure 24: Left: Behaviour of all 21 DAC parameters of ROC1 after the pretest at different temperatures. Right: Mean changes of the 5 interesting DAC parameters of all ROCs.

seen in figure 24 left with the behaviour of the ROC1-DAC parameters after the pretest at different temperatures. Now we concentrate on the 5 DAC parameters that change with temperature: Vana, VthrComp, VoffsetR0, VirefADC and CalDel. The detailed graphs for these parameters are shown in figure 25. One can see that the distribution among the ROCs is very small for VirefADC (new name: PHScale) and VoffsetR0 (new name: PHOffset). There are two outliers for ROC0 and ROC12 at +10°C and -10°C which correspond for both parameters. For Vana the values do not change much for different temperatures: There are fluctuations but no significant temperature dependence. A similar measurement was done by C.Eggel for the old modules in 2009 [6] (page 68) who compared the DAC parameters Vana, VthrComp and CalDel for +17°C and -10°C. The results are shown in figure 24. The two data points of Eggel for Vana indicate a stronger temperature dependence as observed in this experiment. But as there are only two data points one should be carefully interpreting too much in it. The results for the temperature dependence of VthrComp and CalDel show a similar behaviour as the data of Eggel: CalDel gets higher for lower temperatures. VthrComp does not vary much and only shows some fluctuations which agrees with the two data points of Eggel. Interesting is the big range of the observed VthrComp and CalDel values among the ROCs (figure 25). Possibly this has to do with the new Pyxar algorithm which replaced the classical approach of psi46expert.

Finally there are big anomalies in the results of the last measurement at -25°C. It can be seen that the values of VirefADC and VoffsetR0 are at the upper limit (255) which shows that the pulse height optimization has failed. This could be caused by a not converging algorithm which sets CalDel in the Pretest at -25°C to a fixed value (all ROCs have a

very similar value, see figure 25).

There are a few open issues in this chapter. First, more statistics about the temperature dependency of the DAC values for temperatures $>-25^{\circ}\text{C}$ are needed. The tests should be reproduced with different Pretest algorithms, namely P_{xar}. Then the measurement at the setpoint of -25°C have to be redone to verify whether the shown data can be reproduced. If this is the case it would lead in the finding that the ROCs are not efficient at -25°C . If a further test shows different results at this temperatures it is likely that this particular test done in this Semesterarbeit had a problem here, and that there is no issue with the ROCs at -25°C . Furthermore it would be interesting to have information about the temperature dependency on the Trim parameters.

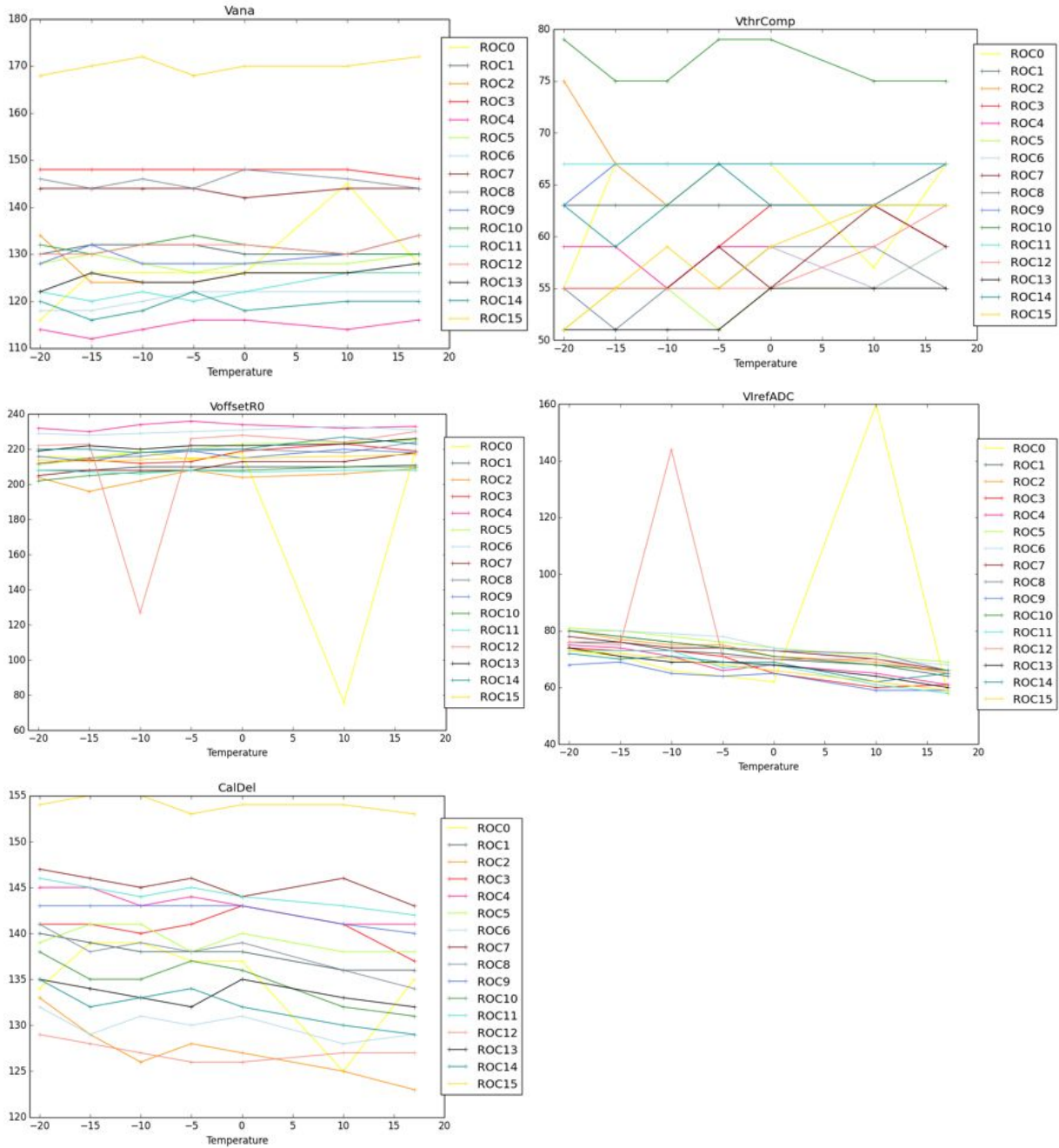


Figure 25: Behaviour of the 5 DAC parameters that change with temperature. Each parameter is shown for every of the 16 ROCs.

6 Conclusion

Thanks to this Semesterarbeit everyone who needs to work with pixel modules in the cold box profits from the detailed temperature maps of the different parts of the setup shown before. It has been observed that the temperature gradient between the cold box base plate and the module base strip is small ($\leq 1^\circ\text{C}$). Little changes to the setup (e.g. varying module positions or changing module holders) do not have a big influence on the temperature distributions. The temperature on the base strips are 0.4°C higher than on

the module holders and the base plate. With powered ROCs the temperature on the base strips are approx. 2°C higher than the temperature on the base plate and the JUMO sensor. With a JUMO setpoint of -25°C the sensor material of the pixel modules get -28.3°C cold and the ROCs are much warmer: They reach a temperature of -22.7°C. The upgraded cold box provides a faster cooling (12 minutes to -20°C; 19 minutes to -25°C) and can cool down to lower temperatures than before. The changes of this upgrade should be considered for any other cold box.

In addition, information was gained about the behaviour of the leakage current at different temperatures. It has been shown that one needs to wait 20 minutes before starting any module test in the cold box after having reached a particular JUMO setpoint. If the box is set to thermal equilibrium, one needs to wait for 5 hours until the leakage current and therefore the sensor temperature gets stable. Moreover, it has been observed that there are five DAC parameters depending on the temperature: Vana, VoffsetR0, VirefADC, VthrComp and CalDel. Big variations have been measured among the ROCs for VthrComp and CalDel. At a setpoint of -25°C big anomalies have been found indicating that either the module is not efficient at this temperature or the Pretest has failed only in this experiment. Furthermore, a step by step guide how to calibrate the silicon sensor temperature was given which can be used for any future experiments in the cold box. With the chosen method of measuring an accuracy of $\leq 1^\circ\text{C}$ on most of the measurements was reached which was satisfying for the shown experiments. The electronic setup with the conductor board and the sensors can also be used for other applications at the IPP.

Some further experiments could expand the knowledge about temperature dependence of pixel modules. First, more experiments concerning the humidity and air temperature in the box would possibly lead to an even stronger proposal to redesign parts of the cooling box. It could also be observed whether the humidity affects module tests. In addition, there should be more tests done concerning the temperature dependence of the DAC parameters. More data is needed to get a more detailed picture of the dependence and the anomalies at -25°C. Also tests of the temperature dependence of the DAC parameters after Trimming are recommended.

All in all this Semesterarbeit gives much information about the temperature and humidity distribution in the cold box, the module testing setup and the modules itself and it lays the foundation of any further investigations in this field.

References

- [1] Lucas Taylor, <http://cms.web.cern.ch/news/tracker-detector>, 2014/05/06
- [2] Lucas Taylor, <http://cms.web.cern.ch/news/silicon-pixels>, 2014/05/06
- [3] Dominguez, A. et al.: CMS Technical Design Report for the Pixel Detector Upgrade. No. CERN-LHCC-2012-016. CMS-TDR-011, 2012.
- [4] Trueb, Peter. CMS pixel module qualification and Monte-Carlo study of H to $\tau^+ \tau^- \text{tol}^+ \text{t}^- \text{ET}$. Diss. Zurich No. 17985, U., 2008.
- [5] B. Kapustka, Cooling Box Commissioning Presentation, 2013/02/06

[6] Eggel, Christina. CMS pixel module qualification and search for B_s^0 to $\mu^+ \mu^-$. Diss. Zurich No. 18232, ETH, 2009.

[7] <http://de.wikipedia.org/wiki/Peltier-Element>, 2014/22/06

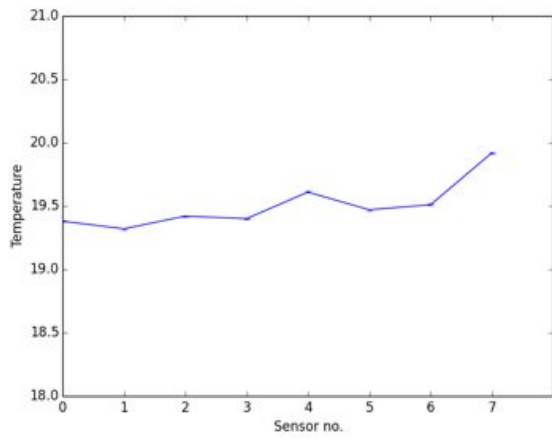
List of Figures

1	The CMS detector. (Source: http://cms.web.cern.ch/news/how-cms-detects-particles ; 5.6.2014)	4
2	Silicon Chip. Source: http://cms.web.cern.ch/news/silicon-pixels	5
3	Experimental setup in the ETH IPP cleanroom.	5
4	Conductor board with Labjack	7
5	Left: Accuracy of used temperature sensors. Right: Accuracy of used humidity sensors with the corresponding label on the sensor.	7
6	Schematic view of the readout of a temperature sensor (above) and a humidity sensor (bottom).	8
7	Left: The old (left) and new (right) water tubes in comparison. Right: The inside of the cold box.	10
8	10 temperature cycles in the new Cooling Box	11
9	Cooling to setpoints -20°C and -25°C	11
10	Left: Humidity sensors in the cold box. Right: Humidity map for setpoint temperature -25°C .	12
11	Left: Temperature map of the air temperature at 4.5 cm above the base plate of the cold box. Right: All measurements of the point in the 4th row from the top, 5th column. No trend can be seen, the measurements fluctuate around a mean value.	13
12	Left: Temperature measurement on the base plate with 7 PT1000 temperature sensors. Right: Temperature map of the base plate at setpoint -20°C .	14
13	Temperature map of the cold box base plate at setpoint -25°C . The measurement points are marked with crosses.	15
14	Temperature distribution of the red module holder in the cold box at position 1 and setpoint temperature -25°C .	15
15	Left: The 3 tested module holders. Right: Exact measurement of red module holder at module position and position 1 in cold box. Setpoint: -25°C .	16
16	Temperature dependence of the yellow module holder on the 4 positions in the cold box.	17
18	Module holder with PT1000 temperature sensor underneath and module on top of it.	18
19	Temperature distribution on module with unpowered ROCs (above) and powered ROCs (below).	19
17	CMS Pixel module. [3] (page 73)	19

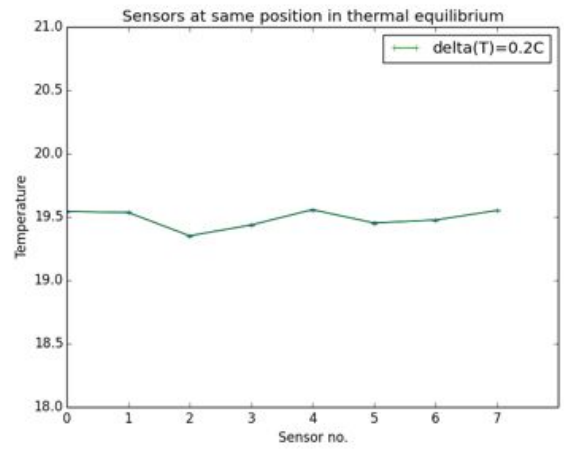
20	Comparison of the temperature distribution on a) the base plate at the area of interest b) the important part of the module holder c) the module base strips with unpowered ROCs c) with powered ROCs. All measurements were done under the same conditions, positions and with a setpoint of -25°C.	20
21	Left: Behaviour of the leakage current in thermal equilibrium with unpowered ROCs. Right: Behaviour at a JUMO setpoint of +17°C with powered ROCs.	21
22	Temperature converted from leakage current, PT1000 underneath the module and JUMO sensor compared at different JUMO setpoints. ROCs power on.	22
23	ROCs first unpowered and then powered. Setpoint: +17°C.	23
24	Left: Behaviour of all 21 DAC parameters of ROC1 after the pretest at different temperatures. Right: Mean changes of the 5 interesting DAC parameters of all ROCs.	25
25	Behaviour of the 5 DAC parameters that change with temperature. Each parameter is shown for every of the 16 ROCs.	27
26	Code to read out the values from Labjack and convert them to temperature/humidity	37
27	Code to create diagrams with leakage current and resistance measurements	43
28	Code to create heatmaps of the cold box base plate	45
29	Code to create heatmaps of the module holder	46
30	Code to create heatmaps of the base strips	47

A Setup

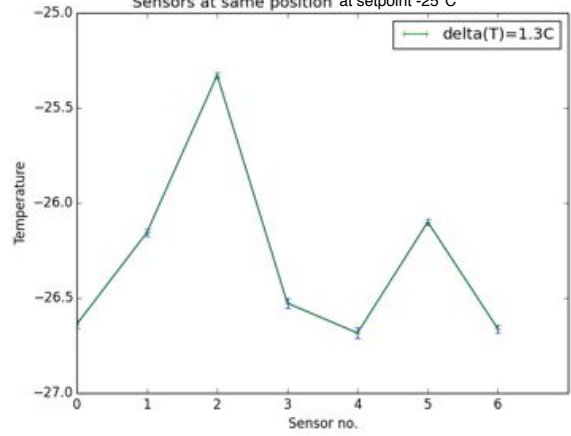
1 Pretest Sensor Calibration of old sensors



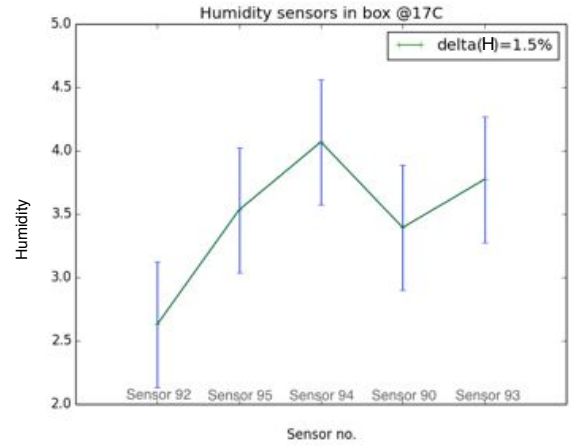
2 Pretest Sensor Calibration of new sensors



3 Sensors at same position at setpoint -25°C

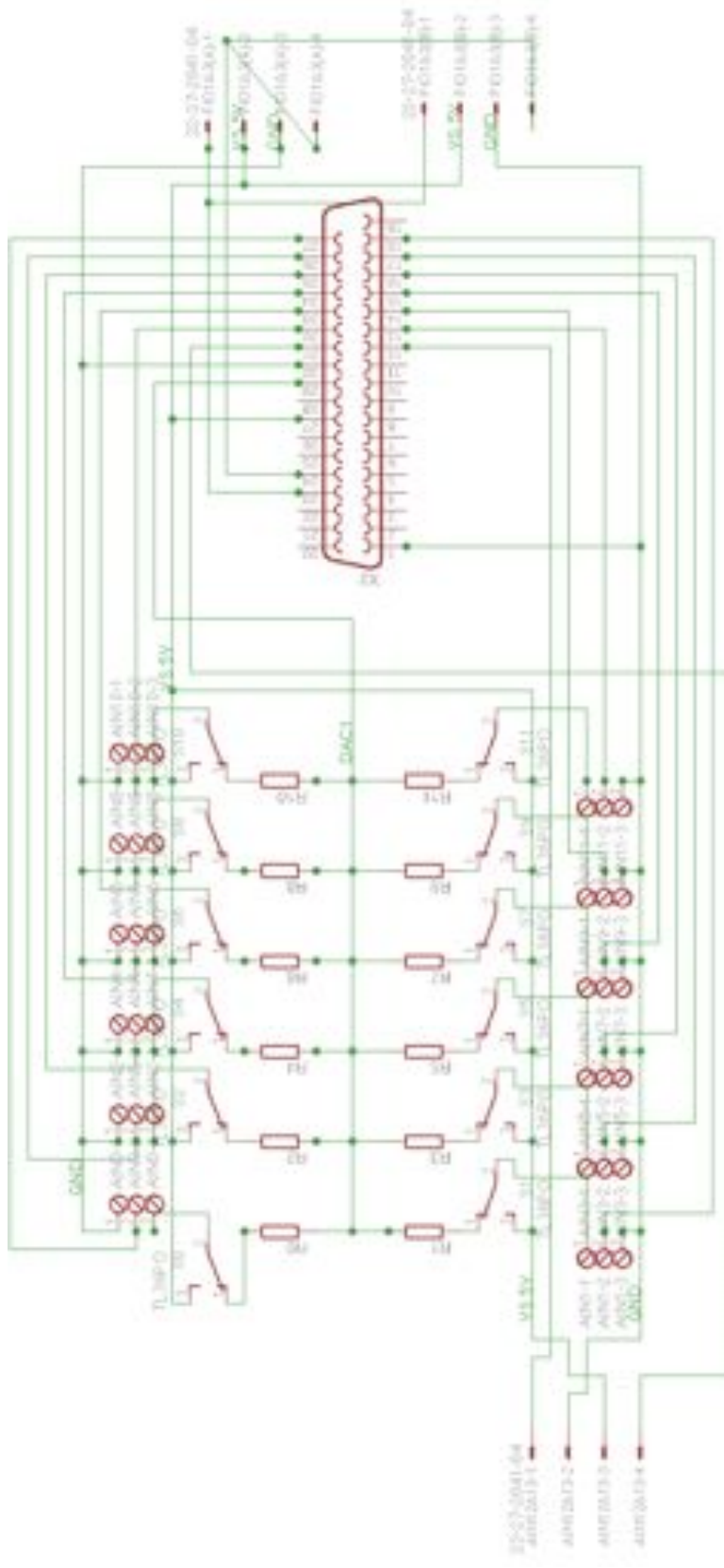


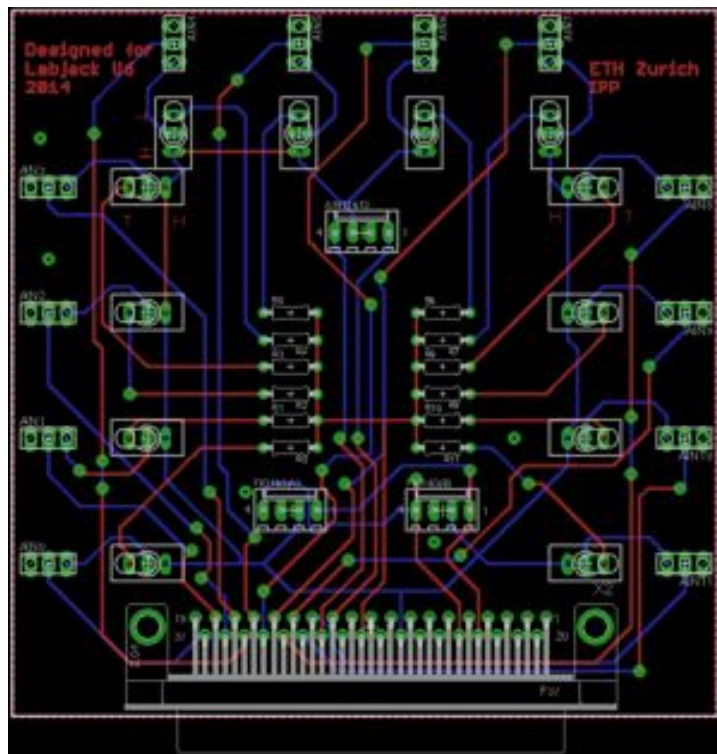
4 Humidity sensors in box @17C



A.1 Conductor Board: Circuit diagram

Circuit diagram of the new circuit board. By
Simon Storz, ETH Zürich IPP, 2014





A.2 Python codes

```
1 import u6
2 import math
3 import numpy as np
4
5 class test:
6     def __init__(self):
7         self.d = u6.U6()
8         self.d.getCalibrationData()
9         self.d.getFeedback(u6.DAC1_8(self.d.voltageToDACBits(.1,dacNumber=1,is16Bits=False)))
10        self.channels_row1 = [12,4,5,3]
11        self.channels_row2 = [1,0,2,6]
12        self.channelth = -1
13        self.resistanceOldplate = {1:995.2,3:995.7,5:996.3,0:995.8,2:996.4,4:994.9,6:996.3,8:1102.5}
14        self.resistance0= {0:995.6,1:995.01,2:994.0,3:994.66,4:994.91,5:995.0,6:995.8,7:995.9,8:996.06,9:994
15        self.HIHa = {90:0.8132,92:0.814,93:0.812,94:0.810,95:0.810}
16        self.HIHb = {90:0.031,92:0.031,93:0.031,94:0.031,95:0.031}
17        self.HIHc = {90:1.0546,92:1.0546,93:1.0546,94:1.0546,95:1.0546}
18        self.HIHd = {90:-0.00216,92:-0.00216,93:-0.00216,94:-0.00216,95:-0.00216}
19        self.supplyVoltage = .1
20        self.channels=[1,2,3,4,5,6,7]
21        self.channels_HIH =[7,8,9,10,11]
22        self.HIHsensors=[92,95,94,90,93]
23        self.nAverage = 150
24
25    def __del__(self):
26        self.d.close()
27
28    def __len__(self,a):
29        return len(a)
30
31    def SetDAC1(self,voltage):
32        self.d.getFeedback(u6.DAC1_8(self.d.voltageToDACBits(voltage,dacNumber=1,is16Bits=False)))
33
34    def get_accurate_AIN(self,channel,Gain=0):
35        feedbackArgument = u6.AIN24(PositiveChannel=channel, ResolutionIndex=13, GainIndex=Gain)
```

Figure 26: Code to read out the values from Labjack and convert them to temperature/humidity

```
36     ainBits = self.d.getFeedback(feedbackArgument)
37     v = self.d.binaryToCalibratedAnalogVoltage(gainIndex=Gain,bytesVoltage=ainBits[0])
38     return v
39     return self.d.getAIN(channel)
40
41 def measure(self,channel0,channels,Rs,nges=10):
42     n= 0
43     Rges=[]
44     Rges2=[]
45     ri=[]
46
47     for i in channels:
48         Rges.append(0)
49         Rges2.append(0)
50     for k in range(0,nges):
51
52         vi = [self.get_accurate_AIN(i,1) for i in channels]
53
54         v0 = self.get_accurate_AIN(channel0,1)
55         print 'v0',v0
56         RT = map(lambda v,R:v*R/(v0-v),vi,Rs)
57         ri.append(RT)
58         Rges = map(lambda x,y: x+y,RT,Rges)
59         Rges2 = map(lambda R,R2: R**2+R2,RT,Rges2)
60         n+=1
61         print n
62     print vi
63
64     mean=map(lambda R: R/n,Rges)
65     print 'mean:',mean
66     np.savetxt('matrixR6.txt', ri)
67     sigma=map(lambda R2,m: math.sqrt(R2/n-m**2),Rges2,mean)
68     return mean,sigma
69
70 def DKRF(self,channelt,channeh,n):
```

```
71     meant0=0.
72     meanh0=0.
73     meant2=0.
74     meanh2=0.
75
76     for i in xrange(n):
77         temp=self.get_accurate_AIN(channelt)
78         meant0+=temp
79         meant2+=temp**2
80         hum=self.get_accurate_AIN(chanelh)
81         meanh0+=hum
82         meanh2+=hum**2
83
84     meant=meant0/n
85     meanh=meanh0/n
86     sigmat=math.sqrt(meant2/n-meant**2)
87     sigmah=math.sqrt(meanh2/n-meanh**2)
88     print meant, sigmat, sigmah
89
90     # Conversion voltage - t and rh
91     t=100./5*meant-20
92     tst=100./5*sigmat
93
94     rh=95./5*meanh
95     rhst=95./5*sigmah
96
97     print "The temperature is: %.3f +/- %.3f C"%(t,tst)
98     print "The relative humidity is: %.3f +/- %.3f"%(rh,rhst), "%"
99
100    self.d.close()
101    return t, rh
102
103    def resistance_to_temperature(self,Ri,sigmaR,r0=1000.):
104        R = Ri/r0*100.
105        t1 =0
```

```
106         sigma =0.
107         if R>=100:
108             alpha = 3.902e-1
109             beta = 5.802e-5
110             t1 = alpha/2/beta-math.sqrt(alpha**2/4/beta**2 - (R-100)/beta)
111             C1 = abs(alpha**2/4./beta**2-(R-100)/beta)
112             sigma=math.sqrt(1/4.*sigmaR**2/beta**2/C1)
113             print 'hallo sigma', sigma
114             print '1',t1
115         else:
116             alpha = 1.597e-10
117             beta = -2.951e-8
118             gamma = -4.784e-6
119             delta = 2.613e-3
120             epsilon = 2.219
121             omega = -241.9
122             t1 = alpha*R**5+beta*R**4+gamma*R**3+delta*R**2+epsilon*R+omega
123             sigma=math.sqrt(sigmaR**2*(epsilon**2+4*delta**2+9*gamma**2+16*beta**2+25*alpha**2))
124             print '2',t1
125         return t1 ,sigma
126
127     def resistances_to_temperature(self,Rs,sigmaRs, r0=1000.):
128         R=np.zeros(8)
129         temp=[]
130         sigmaT=[]
131         print sigmaRs
132         for Ri in Rs:
133             t1,sigma = self.resistance_to_temperature(Ri,sigmaRs[Rs.index(Ri)],r0)
134             temp.append(t1)
135             sigmaT.append(sigma)
136         return temp, sigmaT
137
138     def temp1(self):
139
140         R0=[self.resistance0.get(i,1000) for i in self.channels]
```



```
141
142     self.SetDAC1(self.supplyVoltage)
143     R,sigmaR = self.measure(0,self.channels,R0,nges=self.nAverage)
144     T,sigmaT = self.resistances_to_temperature(R,sigmaR,1000.)
145     # print 'sigmaT', sigmaT
146     print 'T',map(lambda x,y: '%7.2f +/- % 4.2f'%(x,y),T,sigmaT)
147     print 'R',map(lambda x,y: '%7.2f +/- % 4.2f'%(x,y),R,sigmaR)
148     #Array speichern: ANPASSEN!!!!!!!!!!!!!!
149     np.savetxt('T5.txt',T)
150     np.savetxt('sigmaT6.txt',sigmaT)
151     np.savetxt('sigmaR6.txt',sigmaR)
152     np.savetxt('R6.txt', R)
153     self.d.close()
154     return T, sigmaT
155
156 def readHIH2(self,channels,n):
157     Vges=0
158     Vges2=0
159     vi=[]
160     hi =[]
161     for channel in channels:
162         h2 =[]
163         for i in range(n):
164             h2.append(self.get_accurate_AIN(channel))
165         hi.append(h2)
166     Vges=[]
167     Vges2=[]
168     mean=[]
169     sigma=[]
170     for h2 in hi:
171         Vges.append(reduce(lambda x,y:x+y,h2))
172         Vges2.append(reduce(lambda x,y:x+y,map(lambda x: x**2,h2)) )
173         mean.append(Vges[-1]/n)
174         sigma.append(math.sqrt(Vges2[-1]/n-mean[-1]**2))
175     np.savetxt('matrixVAIR6.txt', hi)
```

```
176     print mean, sigma
177     return mean, sigma
178
179     def HIH_to_humidity(self, R, sigmaR, T):
180
181         a=[self.HIHa.get(i,1000) for i in self.HIHsensors]
182         b=[self.HIHb.get(i,1000) for i in self.HIHsensors]
183         c=[self.HIHc.get(i,1000) for i in self.HIHsensors]
184         d=[self.HIHd.get(i,1000) for i in self.HIHsensors]
185         n=len(a)
186
187         rh=np.zeros(n)
188         rhst=np.zeros(n)
189
190     # Humidity conversion + Temperature correction:
191     for i in range(n):
192         rh[i]=(R[i]-a[i])/b[i]*(c[i]+d[i]*T)
193         rhst[i]=(sigmaR[i]-a[i])/b[i]*(c[i]+d[i]*T)
194     return rh, rhst
195
196     def HIH(self, T=23):
197         n=self.nAverage
198         V, sigmaV = self.readHIH2(self.channels_HIH, n)
199         H, sigmaH = self.HIH_to_humidity(V, sigmaV, n)
200         print 'sigmaH', sigmaH
201         print 'H', map(lambda x, y: '%7.2f +/- % 4.2f'%(x, y), H, sigmaH)
202         print 'V', map(lambda x, y: '%7.2f +/- % 4.2f'%(x, y), V, sigmaV)
203         #Array speichern: ANPASSEN!!!!!!!!!!!!!!
204         np.savetxt('sigmaHAIR6', sigmaH)
205         np.savetxt('sigmaVAIR6', sigmaV)
206         np.savetxt('HAIR6.txt', H)
207         np.savetxt('VAIR6.txt', V)
208         self.d.close()
209         return H, sigmaH
210
```

```
1 import matplotlib.pyplot as plt
2 import numpy as np
3 from pylab import *
4 from scipy.optimize import curve_fit
5
6
7 time=np.linspace(0,720,144)
8
9 I = np.loadtxt('IVb.txt')
10 R = np.loadtxt('pt1000b.txt')
11
12 def resistance_to_temperature(Ri,r0=100.):
13     R = Ri/r0*100.
14     t1 =0
15     if R>=100:
16         alpha = 3.902e-1
17         beta = 5.802e-5
18         t1 = alpha/2/beta-math.sqrt(alpha**2/4/beta**2 - (R-100)/beta)
19         C1 = abs(alpha**2/4./beta**2-(R-100)/beta)
20         sigma=math.sqrt(1/4.*sigmaR**2/beta**2/C1)
21         print 'hallo sigma', sigmaR, sigma
22         print '1',t1
23     else:
24         alpha = 1.597e-10
25         beta = -2.951e-8
26         gamma = -4.784e-6
27         delta = 2.613e-3
28         epsilon = 2.219
29         omega = -241.9
30         t1 = alpha*R**5+beta*R**4+gamma*R**3+delta*R**2+epsilon*R+omega
31         sigma=math.sqrt((sigmaR**2/R)*(epsilon**2+4*delta**2+9*gamma**2+16*beta**2+25*alpha**2))
32         print '2',t1
33     return t1
34
```

Figure 27: Code to create diagrams with leakage current and resistance measurements

```
35 def resistances_to_temperature(Rs, r0=1000.):
36     R=np.zeros(8)
37     temp=[]
38     for Ri in Rs:
39         t1= resistance_to_temperature(Ri,r0)
40         temp.append(t1)
41
42     return temp
43
44 def func(x, a,b):
45     return 3.61-a*np.exp(-b*x)
46
47
48 T=np.zeros(len(R))
49 T=resistances_to_temperature(R[:,1],r0=1000.)
50 fig = plt.figure()
51 ax1 = fig.add_subplot(111)
52 t=np.linspace(0,360,20)
53 u=abs(I[180:20000,2]-abs(I[180,2]))/3600
54 I1=abs(I[180:20000,1])*10**7
55
56 y2 = func(u, 1,2)
57 yn = y2 + 0.2*np.random.normal(size=len(u))
58
59 yn=(0,2e-6)
60 popt, pcov = curve_fit(func, u, I1,yn)
61 print popt
62
63
64 plt.plot((I[180:20000,2]-abs(I[180,2]))/3600,I1, '+',u,func(u,popt[0],popt[1]))
65
66 plt.show()
67
```

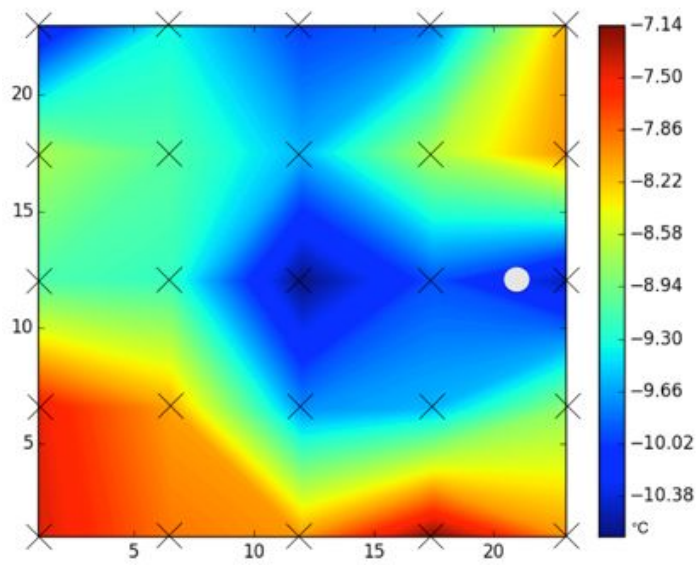
```
1 from mpl_toolkits.mplot3d import Axes3D
2 from matplotlib import cm
3 from matplotlib.ticker import LinearLocator, FormatStrFormatter
4 import numpy as np
5 from pylab import *
6
7 #Files einlesen
8
9 y1= np.loadtxt('HAIR1.txt')
10 y2= np.loadtxt('HAIR2.txt')
11 y3= np.loadtxt('HAIR3.txt')
12 y4= np.loadtxt('HAIR4.txt')
13 y5= np.loadtxt('HAIR5.txt')
14 y6= np.loadtxt('HAIR6.txt')
15 y7= np.loadtxt('HAIR7.txt')
16
17 #Hum Correction:
18 y2[0]=y6[2]
19 y4[0]=y6[3]
20 y5[0]=y6[4]
21 y1[1]=y7[1]
22 y1[2]=y7[2]
23 y1[3]=y7[3]
24 y1[4]=y7[4]
25
26 Z=[y7,y6,y5,y4,y3,y2,y1]
27
28 x = frange(1,25,4)
29 y = frange(1,25,4)
30 X, Y = meshgrid(x,y)
31 contourf(X, Y, Z, 200,vmin=-28.2,vmax=-22.7)
32 colorbar()
33 show()
34
```

```
1 from mpl_toolkits.mplot3d import Axes3D
2 from matplotlib import cm
3 from matplotlib.ticker import LinearLocator, FormatStrFormatter
4 import matplotlib.pyplot as plt
5 import numpy as np
6 from pylab import *
7 import heatmap
8
9 #Files einlesen
10
11 y1= np.loadtxt('T5old.txt')
12
13 z1=np.zeros(3)
14 z2=np.zeros(3)
15 z3=np.zeros(3)
16 for i in xrange(3):
17     z1[i]=y1[i]
18     z2[i]=y1[i+3]
19 z3[1]=y1[6]
20 z3[0]=(y1[0]*1+y1[3]*1+y1[6]*0.62962)/2.62962
21 z3[2]=(y1[2]*1+y1[5]*1+y1[6]*0.62962)/2.62962
22
23 Z=[z1, z3, z2]
24
25 x = [2.4, 4.1, 5.8, 2.4, 4.1, 5.8, 4.1]
26 y = [2.8, 2.8, 2.8, 0.2, 0.2, 0.2, 1.5]
27 imshow(Z, extent=(2.4,5.8,0.2,2.8),vmin=-28.2,vmax=-22.7)
28
29 colorbar()
30 show()
31
```

```
1 from mpl_toolkits.mplot3d import Axes3D
2 from matplotlib import cm
3 from matplotlib.ticker import LinearLocator, FormatStrFormatter
4 import numpy as np
5 from pylab import *
6
7 #Files einlesen
8
9 y1= np.loadtxt('T25poffc.txt')
10
11 z1=np.zeros(3)
12 z2=np.zeros(3)
13 z3=np.zeros(3)
14 for i in xrange(3):
15     z1[i]=y1[i]
16     z2[i]=y1[i+3]
17 for i in xrange(3):
18     z3[i]=(z1[i]+z2[i])/2
19 z3[1]=-24.82
20 z3[0]=(y1[0]*1+y1[3]*1+z3[1]*0.62962)/2.62962
21 z3[2]=(y1[2]*1+y1[5]*1+z3[1]*0.62962)/2.62962
22
23 Z=[z1,z3,z2]
24
25 im= imshow(Z, extent=(2.4,5.8,0.2,2.8),vmin=-28.2,vmax=-22.7)
26
27 colorbar(im)
28 show()
29
30
```


B Measurements

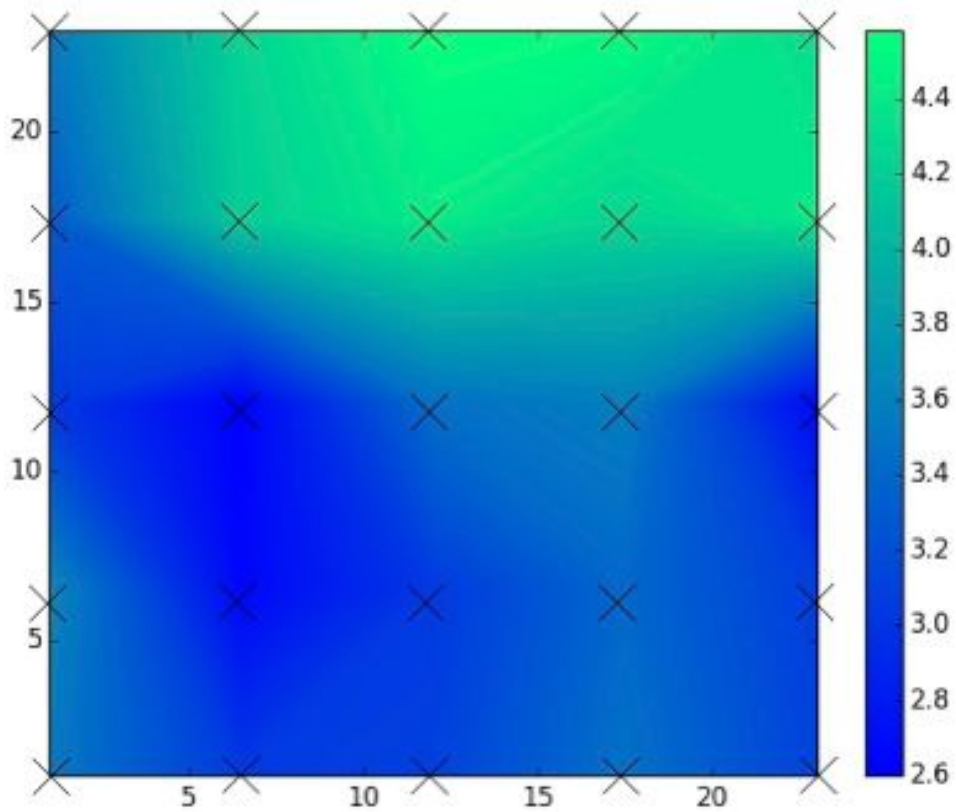
B.1 Humidity and air temperature



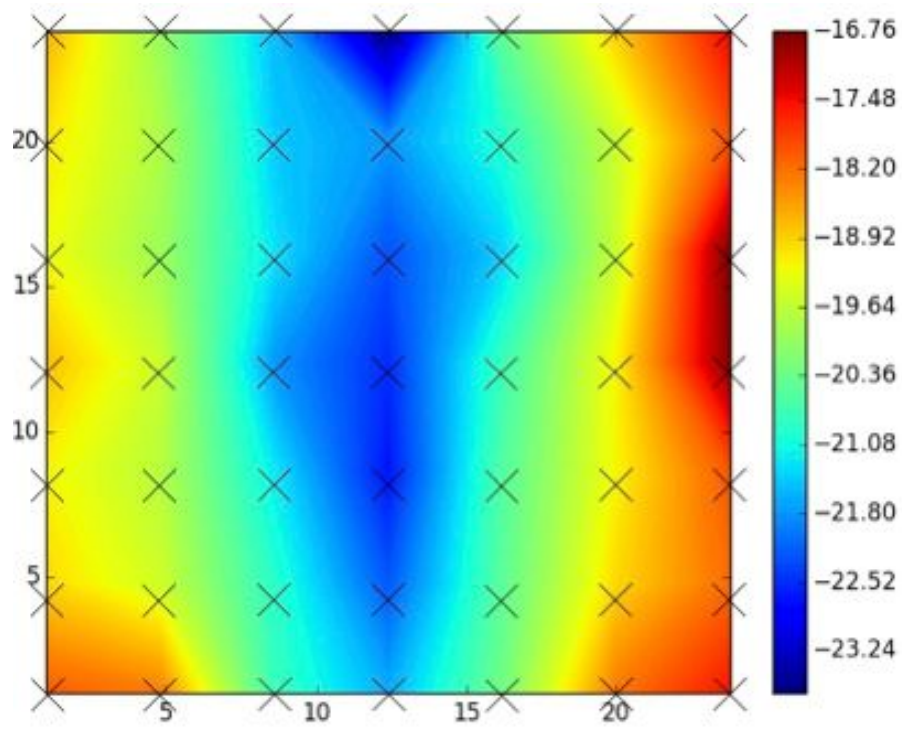
Setpoint -25°C

1 air temperature measured at a height of 4.5 cm in the cold box. set point -25°C

2 Humidity map of 4.5 cm height in the cold box

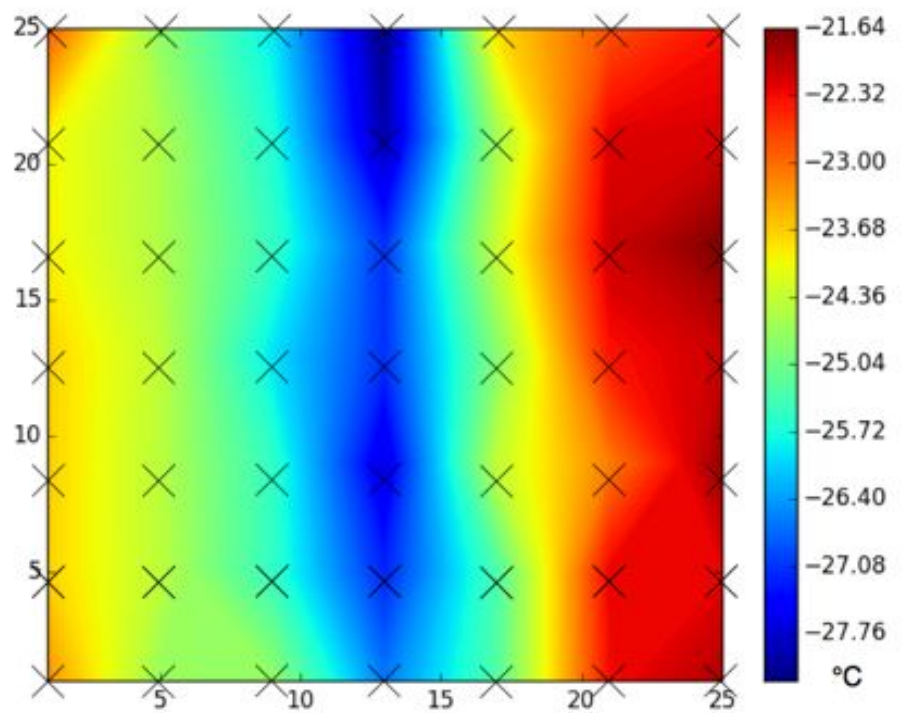


B.2 Base plate



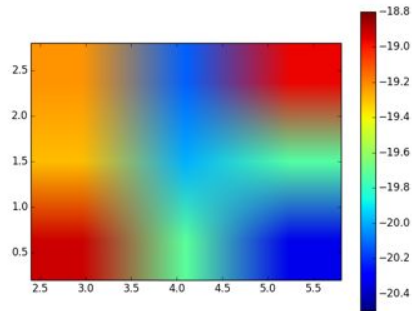
1 Base plate temperature @-20°C

2 Base plate temperature @-25°C



B.3 Module Holder

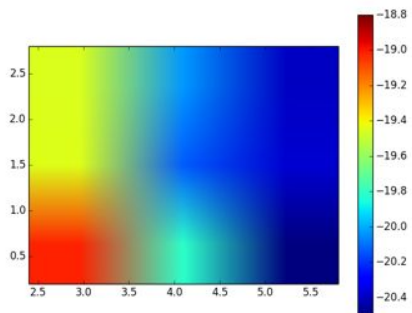
Temperature measurement: Yellow module holder at 4 different positions



0

For all maps:
Measurement
points same as
in pictures in the
thesis.

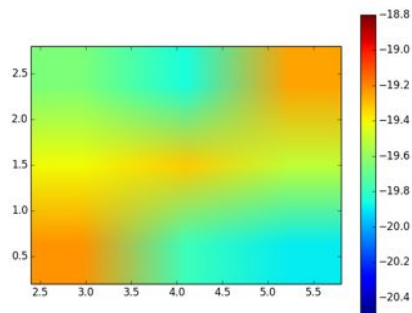
Data points on
the module
holder: (cm)
(0,0) is at the
corner left at the
bottom



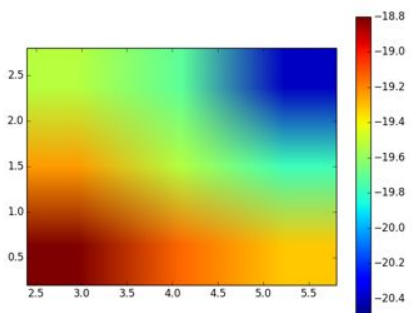
1

x-direction
2.4, 4.2, 5.9,
2.4, 4.2, 5.9,
4.2

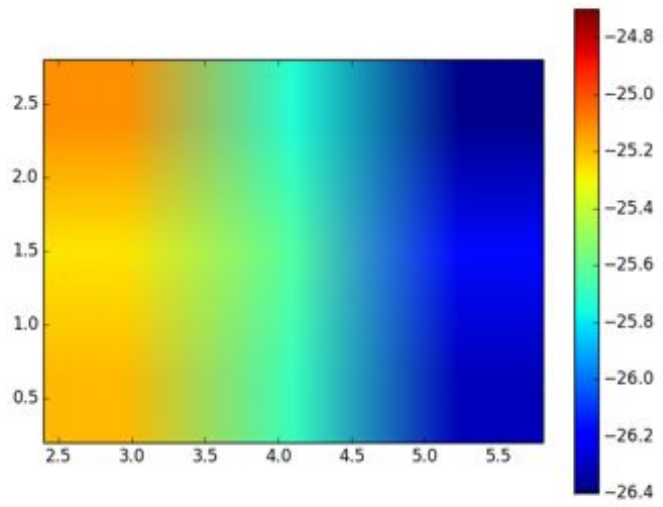
y-direction
2.8, 2.8, 2.8,
0.2, 0.2, 0.2,
1.4



2

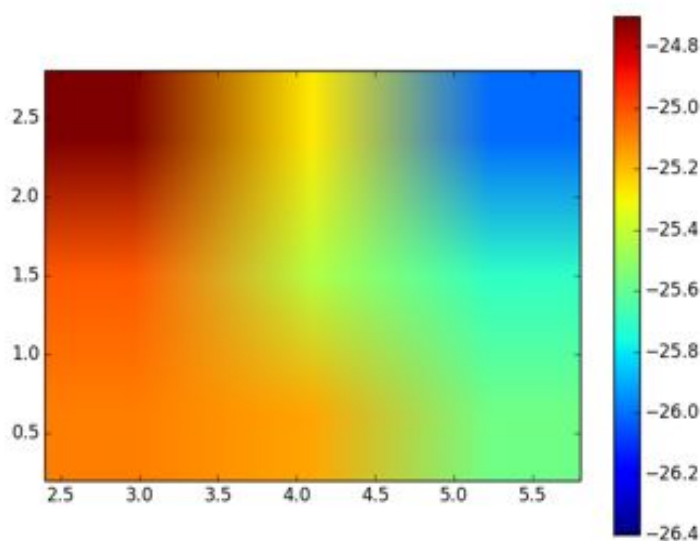
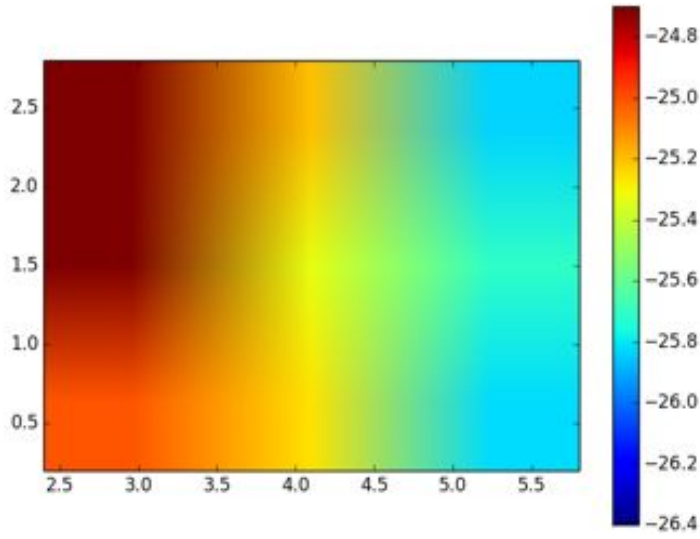


3

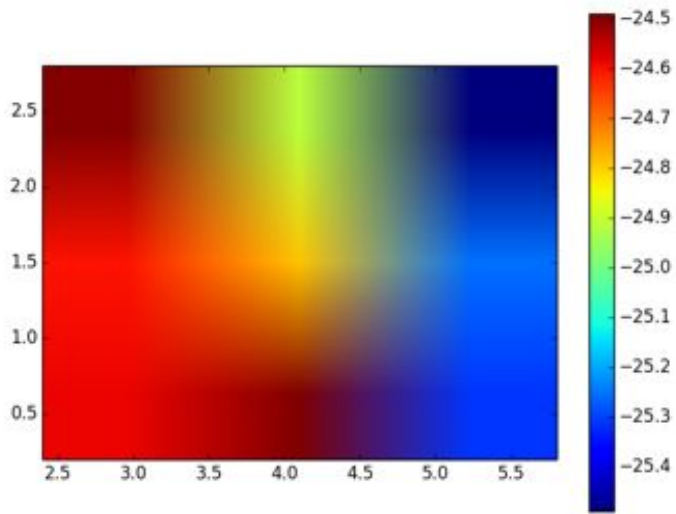


Module holders at module positions:
Setpoint @-25°C, Position 1

- 1 Red holder alone in the box
- 2 Yellow holder alone
- 3 Silver holder alone



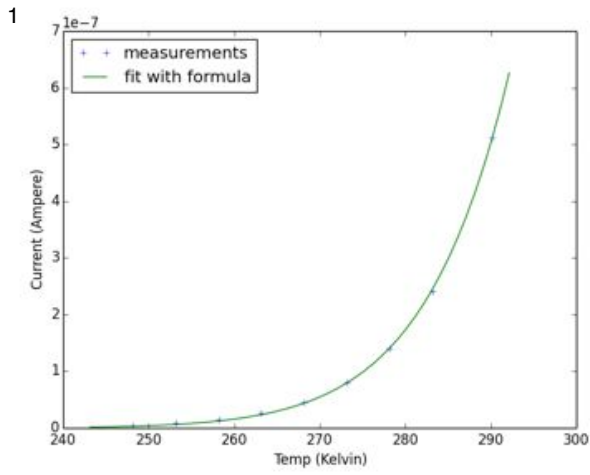
1



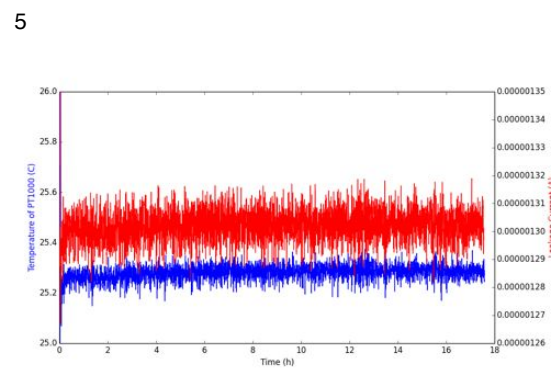
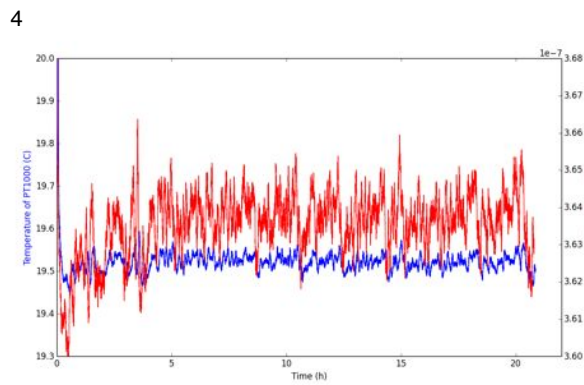
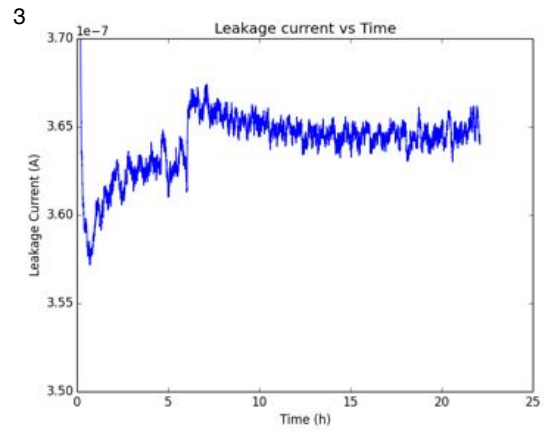
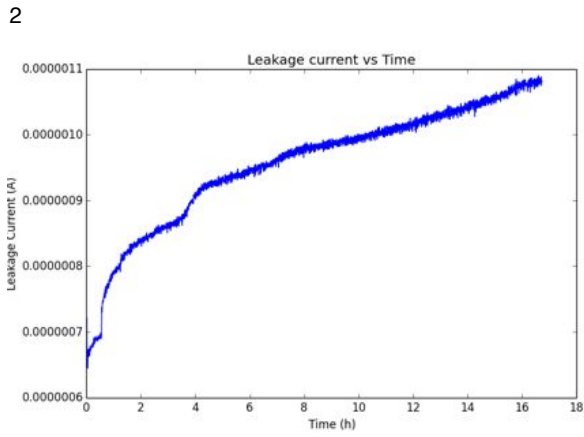
Setpoint -25°C

1 Red module holder with 3 other red holders in the box

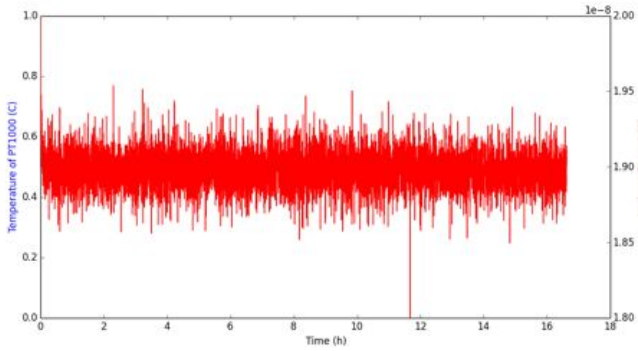
B.4 Leakage current



- 1 Measurement points with fittet formula (7).
- 2 Leakage Current at thermal equilibrium with ROCs on
- 3 Same as 2 with ROCs off
- 4 Same as 3 with additional PT1000 measurement under the module
- 5 Leakage Current at Setpoint -25°C with ROCs on

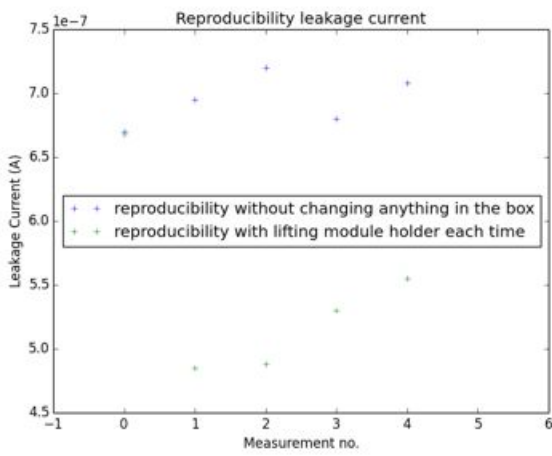


1

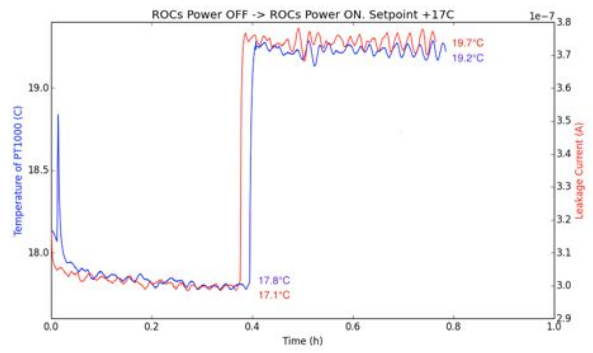


- 1 Leakage Current at setpoint -10°C with ROCs on
- 2 Reproducibility measurements of Leakage Current (ROCs on, thermal equilibrium)
- 3 ROCs off -> ROCs on at setpoint +17°C
- 4 Cycle (ROCs on) at setpoints +17°C, 0°C, -10°C, -20°C, -25°C

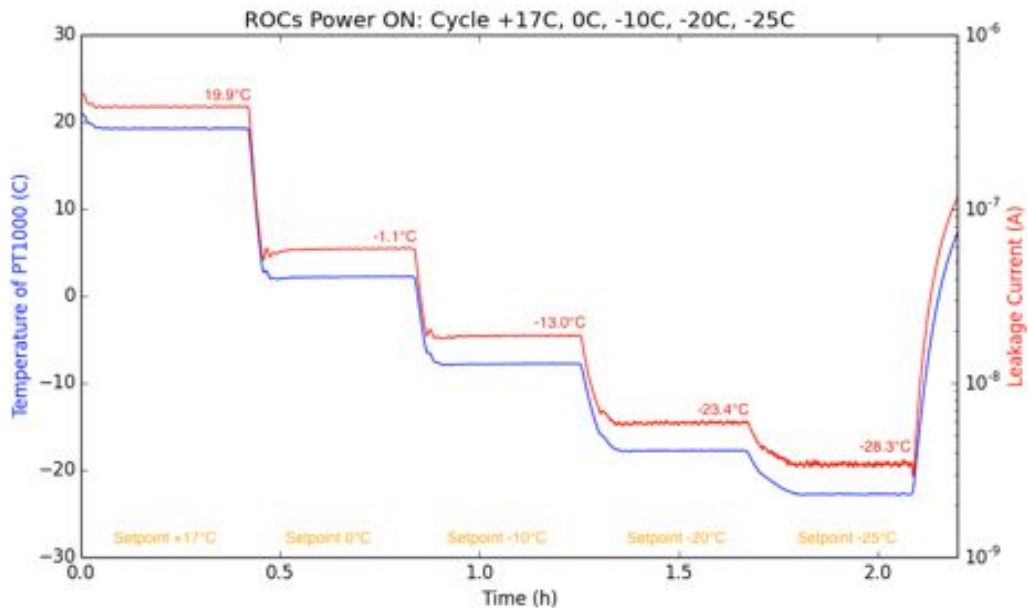
2



3



4



C DAC dependency

DAC dependencies for each ROC for several temperatures

